3 Quantum Chemistry of the Excited State: Recent Trends in Methods Developments and Applications

Miriam Navarrete-Miguel,[a] Javier Segarra-Martí,[b] Antonio Francés-Monerris,[c] Angelo Giussani,[d] Pooria Farahani,[e] Bo-Wen Ding,[f] Antonio Monari,[c] Ya-Jun Liu[f] and Daniel Roca-Sanjuán*[a]

DOI: 10.1039/b000000x [DO NOT ALTER/DELETE THIS TEXT]

Advances (2016-2017) in Quantum Chemistry of the Excited State (QCEX) are presented in this book chapter focusing firstly on developments of methodology and excited-state reaction-path computational strategies and secondly on the applications of QCEX to study light-matter interaction in distinct fields of biology, (nano)-technology, medicine and the environment. We highlight in this contribution developments of static and dynamic electron-correlation methods and methodological approaches to determine dynamical properties, recent examples of the roles of conical intersections, novel DNA spectroscopy and photochemistry findings, photo-sensitisation mechanisms in biological structures and the current knowledge on chemi-excitation mechanisms that give rise to light emission (in the chemiluminescence and bioluminescence phenomena).

1 Introduction

Quantum Chemistry of the (Electronic) Excited State (QCEX) is a field that uses the physical principles of Quantum Mechanics and further concepts particularly developed to efficiently model the chemical processes derived from light-matter interaction or, in general, chemical phenomena involving upper electronic solutions of the Schrödinger equation. QCEX has many applications in biology, (nano)-technology, medicine and the environment, in which the population of the excited electronic states gives rise to chemical phenomena not allowed in ground-state chemistry. E/Z double-bond isomerisations, [2+2] cycloadditions, charge transport, tautomerisations or luminescence are examples of such rich chemistry. Here, multi-radicaloid structures, energy degeneracies between distinct configurations of the electrons, intra-molecular or inter-molecular charge transfer (CT) are common features of the excited electronic states which allow the mentioned chemistry.

In our previous biannual contributions to the RSC Photochemistry Specialist Reports,[1,2,3,4] we have reviewed the advances on quantum-chemistry computational studies focusing on photo-induced chemical processes and also on the phenomena arisen as the result of a chemical reaction (chemiluminescence (CL), bioluminescence (BL) and dark photochemistry). We have traditionally organised the work in two parts firstly describing methods developments and next analysing the trends observed in the application of QCEX. We shall continue here with such style. For the first part, taking into account the publications in 2016 and 2017, we find convenient this time to split the section into three parts separating static electron-correlated methods, dynamic electron-correlated methods and

methodologies or computational strategies to obtain dynamical properties.

QCEX requires multiconfigurational approaches able to describe on the same foot distinct configurations of the electrons around the nuclei (or configuration state functions) which usually appear in excited states with similar energies. The interaction of such energetically-close configurations gives rise to the so-called static (also strong or long-range) electron correlation. A representative method able to compute the static correlation is the complete-active-space self-consistent field (CASSCF), in which a group of chemically-relevant orbitals is chosen and all possible electronic configurations arisen from distributing the active electrons over those active orbitals are allowed to interact in the computational procedure. Such strong-correlated methods provide a correct wavefunction for the excited state, however, the obtained energies are far from accurate. Short-range interaction between electrons (dynamic correlation) is still needed for an accurate energy determination. In this context, a practical and general strategy in the particular case of the CASSCF method is to use second-order perturbation theory for such purpose, giving rise to the complete-active-space second-order perturbation theory (CASPT2) method.

CASSCF/CASPT2 and other multiconfigurational methods allow therefore for an accurate determination of the excited-state electronic-structure properties, which is a big step although not enough. Excited-state chemistry determinations additionally require computational strategies able to determine the accessible and relevant excited-state chemical paths. Minimum-energy path (MEP) computations are accurate procedures providing a static description based on energy barriers. A further step implies determining excited-state time-dependent properties such as lifetimes or photochemical rates, which is a complex and computationally costly task. Nevertheless, since some years ago, advances in computer hardware, QCEX methods and software have allowed to modestly address such problems. Many scientists in the field are therefore spending efforts to improve and apply such dynamical computational approaches.

Regarding applications of QCEX, adiabatic and non-adiabatic chemistry can be distinguished. Whereas the former, similarly to the ground-state chemistry, involves only one electronic state (even though this can be formed by many electronic configurations), the latter normally refers to non-radiative changes between two (or more) states. In QCEX, such non-adiabatic chemistry is associated with conical intersections (CIXs) and singlet-triplet crossings (STCs), which are related to internal conversion (IC) and intersystem crossing (ISC) phenomena, respectively. As can be seen in our previous reports, CIXs and STCs are crucial in many phenomena of light-matter interaction of relevance in fields such as DNA damage, organic photovoltaics, luminescence materials or BL. We shall include in this chapter a section dedicated to recent trends on the roles of CIXs and STCs. The other sections shall describe advances on DNA spectroscopy and photochemistry, photosensitisation mechanisms in biology and medicine and CL and BL.

2 Developments of methods and theory

Over the last couple of years plenty of novel advances have been made in the field of theoretical chemistry focused on the accurate characterisation of electronic excited states. Most theoretical developments and implementations can be roughly separated in two markedly different research avenues, namely those dealing with an

improved description of the so-called static (or strong) correlation and those focusing on efficient ways to include the remaining dynamic correlation. Static correlation manifests itself as a significant deviation of the correlated electron density from the one given by the Hartree-Fock approximation and is often localised in a small portion of the molecule (e.g. metals and nearby ligands in transition metal complexes). This rationale is widely used in CASSCF methods that represent a suitable choice of the mean-field approximation due to its multiconfigurational character and where only dynamic correlation is then missing.[5, 6] Dynamic correlation, on the other hand, is an extensive quantity with respect to the size of the system, and its evaluation becomes very costly for large molecules. This is mainly due to its slow convergence with respect to the amount of molecular orbitals included, which results in a large increase in the computational demands for quantitative analysis even for small to medium-sized systems when using diffuse and accurate basis sets. These two different kinds of correlation have thus attracted much attention over the last few years and reviewing them will be the focus of the first two sub-sections. It is worth noting, however, that widely used methodologies such as time-dependent density functional theory (TD-DFT) have been omitted from this review as we focus on wave function-based *ab initio* approaches to correlation, the interested reader is pointed towards some recent works that illustrate the state-of-the-art of this particular field.[7, 8, 9]

2.1 Methods: Static (strong) correlation

A surge in the use of methods accounting for static correlation has been witnessed over the last few years and is mainly due to a range of schemes that have become available for solving the full configuration interaction (FCI) problem in wave function-based multiconfigurational techniques, which is the main bottleneck of CASSCF-like methods. These could roughly be separated in a few different strategies, with those based i) on density matrix renormalisation group-based (DMRG)[10, 11, 12] techniques, ii) FCI quantum Monte Carlo (FCIQMC) methods,[13, 14, 15] and iii) semi-stochastic Heat-bath Configuration Interaction (HCI)[16, 17] being among the most relevant and followed approaches. A schematic view of these different schemes is given in Figure 1. These different techniques are grounded on quite diverse principles, which will be very briefly summarised next, the reader being referred to the original citations given above for a more detailed account. DMRG focuses on incorporating locality to describe the strong correlation problem as is schematically shown in Figure 1a top and middle panels, where the sequence of contractions of the auxiliary indices in the DMRG in its matrix product state formalism for the wave function are shown, which induce local correlation and allow for efficient evaluations of expectation values. Figure 1a lower panel, on the other hand, displays the matrix product form of the states and their overlap, which allows for decomposing the overlap itself as a series of overlaps associated with each localised site and facilitates the computation of expectation values and the application of the variational principle on top of such wave functions.[18] DMRG-based algorithms are the oldest and most featured, having been recently implemented within the second-order CASSCF solver[19, 20] algorithm initially devised by Werner and Knowles[21] and also been extended to restricted/complete active space state interaction (RASSI/CASSI)[22, 23] formulations similar to those previously introduced for standard CASSCF/RASSCF implementations,[24, 25] which allow

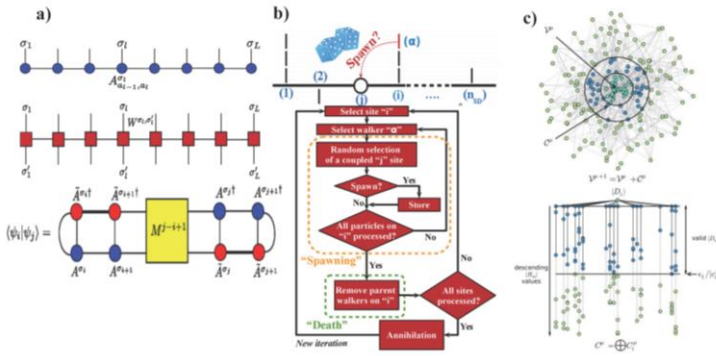

Figure 1. Scheme of the different FCI solvers recently developed to tackle the static correlation problem and featuring a) DMRG, b) FCIQMC and c) HCI. Panel a) is reproduced from *Phys. Rev. B*, 2017, **95**, 064110 with permission from the American Institute of Physics, panel b) reproduced from *J. Chem. Theory Comput.*, 2016, **12**, 1245 with permission from the American Chemical Society, and panel c) reproduced from *J. Chem. Theory Comput.*, 2017, **13**, 5468 with permission from the American Chemical Society.

obtaining essential magnitudes such as oscillator strengths. FCIQMC relies, on the other hand, on finding a solution to the FCI problem through stochastic means. The key point of FCIQMC is that instead of allocating memory for accommodating the entire FCI vector, as often done in standard implementations, only determinants significantly populated along the Monte Carlo sampling (based on a hash algorithm that communicates all walkers or particles used to this purpose, schematically represented in Figure 1b) are stored so that the many determinants not contributing prominently can be excluded, allowing for much larger active spaces to be feasible. HCI is similar to FCIQMC in that it uses the concept of removing many of the determinants that do not significantly contribute to the wave function, but it does so by following a different path. In this case, the selected configuration interaction method is initially used to pick only the important determinants in the active space (scheme given in Figure 1c), which is then improved by performing perturbation theory on top of those. HCI brings in a semistochastic implementation that heavily increases the efficiency of the Epstein-Nesbet perturbation theory treatment while also improving the variational stage of the method. In this way, HCI differs from the methods previously outlined in that it also provides estimates of the dynamic correlation energy, neglected in CASSCF-like methods and where dynamic correlation is often included *a posteriori* with a range of different techniques that will be covered in the next section.

One weakness of these methods often mentioned in the literature is the need to define an active space or set of orbitals in which the FCI or similar treatment will be performed given the present inability of running such schemes over the whole molecular orbital space. The choice of the active space is indeed important and requires certain prior knowledge of the system under study and of the method itself,[26, 27] which can prove to be an insurmountable barrier for non-specialist users. Nevertheless, encouraging recent developments have shown different ways in which active spaces might be automatically selected in a black-box manner,[29, 28] enabling

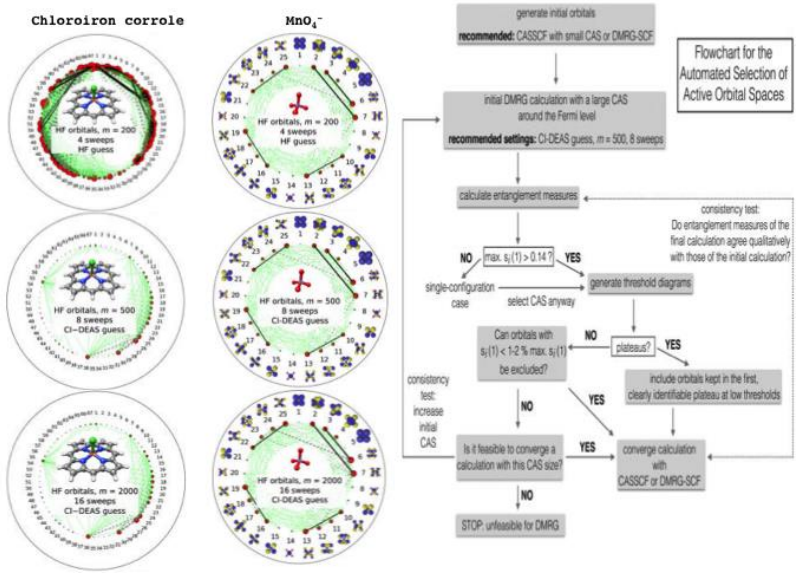

less experienced researchers to make use of these highly correlated techniques.

Figure 2. Automatic active space selection algorithm described by Stein and Reiher.[29] Figure reproduced from reference 29 with permission from the American Chemical Society.

Figure 2 shows an example of such an algorithm recently devised by Stein and Reiher[29] where a systematic selection procedure is depicted for DMRG, and where a range of initial guesses are shown to yield analogous results thus demonstrating its robustness and thus being suitable for applications in a black-box fashion.

Many other developments have been carried out within static correlated methods based on the original implementations that still rely on a Davidson-like solver for the FCI problem. Martínez and co-workers have developed a graphical processing unit (GPU)-based algorithm for CASSCF [30] including its non-adiabatic coupling framework[31] that exploits the massive parallelisation offered by these state-of-the-art technologies. They have also explored efficient approximations to CASSCF such as the floating occupation molecular orbital-complete active space configuration interaction (FOMO-CASCI) within GPU technologies,[32, 33] which comes at a cost similar to TD-DFT while being able to represent states with a sizeable multiconfigurational character. Significant advances have also been made with respect to the more efficient treatment of the two-electron integrals handled by these algorithms *via* the Cholesky decomposition, which vastly increases the number of basis set functions and hence allows for larger and more precise basis sets to be employed.[34, 35, 36]

These are but a few representative examples that display the overall trends followed in the field, which can be summarised in the following points: i) alternative and more efficient FCI solvers are being pursued to correlate more orbitals and thus extend the use of statically correlated methods to large scale applications, ii) methods are being introduced to remove the potential bias of selecting the active

space by providing a robust automated active space selection algorithm transitioning these methods to a black-box fashion, and iii) novel technologies such as GPUs and more sophisticated two-electron integral schemes are being adopted to increase their computational efficiency.

2.2 Methods: Dynamic correlation

Plenty of advances have been reported over the last couple of years for including more effectively dynamic correlation. Here we will survey recently developed techniques to include dynamic correlation on top of statically/strongly correlated (multiconfigurational) methods. These will be split on those based on i) CASPT2,[37] ii) N-Electron Valence state perturbation theory (NEVPT2),[38] iii) density functional theory (DFT) on top of multireference wave functions and iv) coupled-cluster based theories.

The first type to be reviewed will be the CASPT2 method,[39] which consists on a multiconfigurational variant of second-order Møller-Plesset perturbation theory on top of a CASSCF reference wave function. A revived interest in the CASPT2 method has been witnessed in recent years due to the possibility of overcoming previous limitations associated to its elevated computational scaling. To this end, formulations of the Pair Natural Orbital (PNO)-CASPT2[40] and the Frozen Natural Orbital (FNO)-CASPT2[41] have been reported, providing massive speed-ups that enable its use with larger basis sets and larger molecular systems. A novel extrapolation scheme has also been proposed,[42] whereby the Shanks extrapolation method can be applied by combining several low-cost FNO-CASPT2 (and potentially other similar techniques such as PNO) computations to extrapolate the exact total energy. Shiozaki and co-workers have reported outstanding work on the derivation and implementation of analytical fully internally contracted CASPT2 energy gradients[43, 44] and non-adiabatic couplings,[45] which enable their long sought use for on-the-fly non-adiabatic MD schemes as those that will be discussed over the next section. The CASPT2 method has also been recently extended to work within the Generalised Active Space (GAS) framework leading to the GASPT2 method,[46] which is a cost-effective alternative of CASPT2 where only a few selected excitations are allowed within the active space dramatically reducing its cost. DMRG variants of the CASPT2 method[47] and its multistate (MS-CASPT2)[48] extension have also been recently reported, allowing the accurate determination of electronic excited states with unprecedently large active spaces.

NEVPT2 will be reviewed next, being a very similar method to CASPT2 with the exception that it employs a two-electron Dyall Fock operator that drastically reduces some of the known problems of CASPT2 such as intruder states and the need to use further corrections for treating open-shell systems (IPEA shift).[49] Very efficient novel implementations of the NEVPT2 method have been recently reported, featuring its explicitly correlated (F12)[50] variant and the domain based localised pair natural orbital (DLPNO)[51] among them, which enable the use of NEVPT2 for very large systems and diffuse basis sets. Two different implementations within a DMRG framework have also been recently reported for its partially contracted form,[52, 53] as well as one within its strongly contracted scheme,[54] which refer to different levels of contraction used in the formulation of the zeroth-order Hamiltonian employed. These advances are particularly relevant for transition metal complexes where the double-d shell effect[55] forces the inclusion of a large amount of orbitals to the active

space in order to provide converged results. A new time-dependent variant has also been introduced for both DMRG-based[56] and Matrix Product State (MPS)-based[57] wave functions that displays lower scaling than the strongly contracted NEVPT2 method while providing energies analogous to those of the fully uncontracted form, which should greatly improve the applicability of the method for large-scale applications. Finally, two different implementations for the internally contracted NEVPT2 have been devised within the MPS framework,[58, 59] displaying the huge advances made within N electron valence perturbation theory combined with state-of-the-art DMRG-based methodologies and being favoured in many cases to the more popular CASPT2 method.

Another way to include dynamic correlation on top of a statically correlated wave function is to employ DFT, which is known to feature a very favourable scaling and thus provide an efficient and accurate characterisation of the remaining correlation missing combining the advantages of wave function and DFT. To this end, many different approaches have been recently devised and will be surveyed next. The first is the pair-DFT, which is based on a generalisation of Kohn-Sham DFT where the electron kinetic and classical electrostatic energies are computed from a reference wave function and the rest of the energy is obtained from a density functional.[60] The main differences with standard Kohn-Sham DFT approaches are the use of a multiconfigurational reference instead of a single Slater determinant and that the density functional is in this case a function of the total density and the on-top pair density instead of being a function of spin-up and down densities. This method has been successfully applied in a number of difficult cases and has been shown to provide reliable results thus making it a promising technique in the field of theoretical photochemistry. The next method is based on the short-range formulation of DFT (srDFT)[61] and uses the same framework previously described making use of a multiconfigurational wave function while exploiting the advantages of DFT for adding the remaining dynamic correlation. In this case, this is done by capitalising on the efficient treatment of the short-range dynamical correlations provided by a number of recent DFT developments and approximations. Another efficient way to include correlation on top of a statically correlated wave function, of multireference configuration interaction (MRCI) nature in this case, is described next thorough the advances in the DFT/MRCI[62, 63] method recently developed by Marian and co-workers. These implementations build on the original work of Grimme and Waletzke[64] and improve this well-established semi-empirical quantum chemistry method by producing a redesign of the original Hamiltonian which fixes some of its known problems such as the inability to treat bi-chromophores due to the strong dependence of the parameters used in the Hamiltonian for describing the different excitation classes. Marian and co-workers provide a new parameterisation that is spin-invariant and incorporates a lesser amount of empirical parameters compared to the original formulation,[62] which has also been recently extended to treat open-shell systems.[63] The last technique combining a multiconfigurational reference and DFT is the ensemble DFT approach.[65] The approach is based in considering an ensemble of ground and excited states like in statistical physics, where the ensemble is characterised by the total number of states and their respective weights, and that can be employed in order to simulate electronic excited states in a time-independent manner while considering a certain degree of strong correlation.

The last group of techniques reviewed encompasses coupled cluster and the

different advances made to both its use on top of multiconfigurational wave functions as well as the recent improvements made in single determinant formulations to treat potential energy crossing regions. A PNO formulation has been recently presented,[66] which allows the characterisation of electronic excited states at a vastly reduced cost by using the back-transformed PNOs within the framework of equation of motion coupled cluster theory and its similarity transformed variant. A derivation for equation of motion coupled cluster analytical non-adiabatic couplings is also to be highlighted,[67] as this would in principle allow the use of these extremely accurate techniques for non-adiabatic dynamics simulations. Despite the availability of analytical couplings, the question still remains in whether single Slater determinant-based methods such as these can indeed be reliable for properly representing inherently multiconfigurational regions of the potential energy surface (PEH) such as interstate crossings (CIXs). Koch and co-workers report some encouraging results in this regard by presenting a novel specific formulation of coupled cluster theory that correctly describes conical intersections between electronic excited states of the same symmetry,[68, 69] which should in principle allow for their use in photo-excited MD. Lastly, a DLPNO formulation of Mukherjee's state-specific multireference coupled cluster method has also been recently reported,[70] providing huge speed-ups for these lengthy simulations and bridging the gap towards their routine use in real applications.

The list of recent advances outlined above is by no means exhaustive and represents mostly the different paths taken in order to include dynamic correlation on top of multiconfigurational reference wave functions. These can be summarised as follows: i) perturbation theory-based methods (CASPT2 and NEVPT2) remain the most popular due to their favourable scaling, ii) DFT corrections on top of multiconfigurational wave functions appear to be increasing in popularity due to being even more efficient computationally than those based on perturbation theory, and iii) encouraging advances are being made on the coupled cluster front in order to reduce its cost and make it affordable for medium-sized systems as well as to be able to represent crossing regions properly to enable its use in theoretical photochemistry.

2.3 Dynamics

During the years 2016 and 2017, significant developments in the field of dynamics simulations of photophysical and photochemical processes have been achieved. We shall focus here on achievements on quantum dynamics, and in particular, progresses which have been made regarding on-the-fly quantum dynamics simulations, the possibility of describing states of different spin-multiplicity (as singlet and triplet states), a first non-adiabatic MD method based on the exact factorisation of the electron-nuclear wave function and a promising improvement of the efficient multi-layer multiconfigurational time-dependent Hartree (ML-MCTDH) approach based on an adaptively expansion of the number of single-particle-functions during the dynamics.

On-the-fly dynamics methods are those that do not require the knowledge of the PEH before the dynamics can be run, but instead, as the name suggested, the required regions of the PEHs are computed only when needed (*i.e.* on-the-fly) along the dynamics, normally through the interface with an external electronic structure theory program. On-the-fly methods are particularly attractive, since they circumvent one of the main bottlenecks in performing quantum dynamics that is the need of computing beforehand the various PEHs, a task that becomes quickly computationally prohibitive with the increase of the number of degrees of freedom.

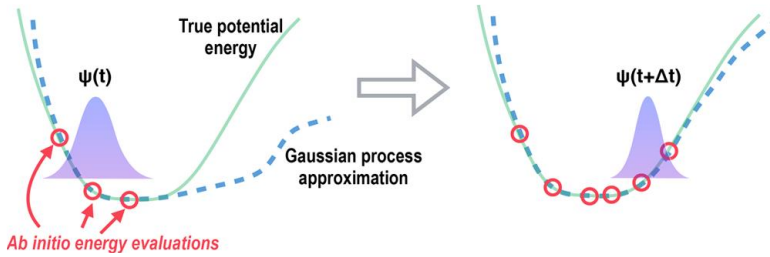

Figure 3. Pictorical representation of the GPR introduced by Richings and Habershon. Reproduced from *J. Chem. Theory Comput.*, 2017, **13**, 4012 with permission from the American Chemical Society.

Among on-the-fly dynamics simulations, the direct dynamics variational multiconfigurational method (DD-vMCG) stand out for being a full quantum dynamics method, in which both the basis functions used for expanding the nuclear wave function and the corresponding coefficients evolve according to a variational resolution of the nuclear time-dependent Schrodinger equation (TDSE). DD-vMCG is consequently in principle able to correctly describe quantum effects as tunnelling and non-adiabatic processes. Since quantum dynamics are normally run along diabatic states, and since electronic structure theory programs provide instead adiabatic states, a diabatisation procedure is needed in order to run DD-vMCG dynamics. The propagation diabatisation method was previously presented and used in conjunction with DD-vMCG dynamics, and in 2017, the work of Richings and Worth extended its applicability, previously restricted to only two states, to an arbitrary number of states.[71] This diabatisation scheme is based on the propagation of the adiabatic/diabatic transformation matrix K, and its relationship with the matrix of non-adiabatic couplings term (NACT) vectors, F, which is: $\dot{K}=-FK$. The equation, strictly exact only in the limit of a complete electronic basis set, allows to propagate the K matrix to the subsequent point in the dynamics ($R+\Delta R$) from the knowledge of K at the initial point (R) and the integration of the F matrix along the path from R to $R+\Delta R$. Richings and Worth used the propagation diabatisation scheme for running DD-vMCG dynamics on the butatriene cation and on thymine, including in both cases a variable number of excited states. The results proved the applicability of the propagation diabatisation scheme and shown how the number of states included in a DD-vMCG simulation influences the outcomes of the dynamics in terms of population transfer and wavepacket spread.

In all on-the-fly dynamics simulations a local approximation of the PEHs based on the actual points computed on-the-fly by the electronic structure theory program must be performed. In 2017, Richings and Habershon presented a method called Gaussian process regression (GPR) for an efficient construction of a global PEH from *ab initio* electronic structure calculations at selected configurations (see Figure 3).[72, 73] According to the GPR method, the PEH is represented by a linear combination of Gaussian functions, centred at a set of M reference points in configuration space. The weights of such an expansion are determined imposing the equality between the approximate PEH and the computed reference points. Initially, a fixed number of reference points are a predefined sampling subspace. New reference points are then added along the dynamics,

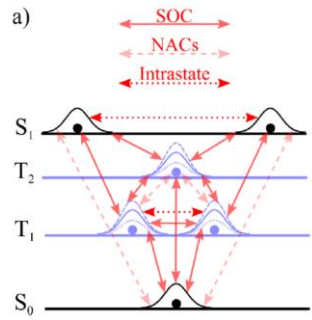

Figure 4. Pictorical representation of all possible coupling between trajectory basis functions included in the GAIMS method. Reproduced from *J. Chem. Phys.*, 2016, **144**, 101102 with permission from the American Chemical Society.

originated by a random uniform sampling for each degree of freedom within the limits of exploiting the fact that GPR allows the evaluation of the accuracy of the approximated PEH at any point without having to calculate the actual PEH. It is in fact possible to compute the variance at any point, which in turn reflects the accuracy of the PEH based on the expansion derived by the current set of reference points, and can consequently be used in order to decide whether or not compute and add the new geometry to the reference points. A second strength of GPR is that it can provide an approximate PEH having a sum-of-products form, which is the form required for MCTDH simulations, consequently making GPR suitable for running MCTDH simulations without the need to precompute the PEH. Richings and Habershon tested the GPR method on the butatriene cation, and on reduced models of malonaldehyde and salicylaldimine.

Most of the available quantum dynamics approaches are able to account for non-adiabatic transitions only among states of the same spin-multiplicity, with only semiclassical methods as trajectory surface hopping (TSH) offering the possibility of describing ISC processes. So, despite the recognised importance in many photoinduced processes of the interplay between singlet and triplet states, spin-orbit couplings (SOCs) and the resulting ISC processes were not included in most dynamics simulations. Things have improved since 2016, year in which two independent publications presented an extension of the Ab-Initio Multiple Spawning (AIMS) method able to describe the interaction between states of different spin-multiplicity.[74, 75] In both works, the Hamiltonian appearing in the AIMS equation of motion for the wave-function amplitudes now includes a SOC part, added to the usual spin-free electronic Hamiltonian and the nuclear kinetic operator. In such a way the off-diagonal elements of the Hamiltonian between two spin-diabatic electronic states having different spin multiplicity are equal to the corresponding SOC. The latter can be computed along the dynamics using the first-order saddle-point approximation, which is here particularly justified by the smooth change that the SOC describes with respect to the nuclear position. In line with AIMS philosophy, when an ISC process from state I to J is considered to be likely, the phenomenon is described by creating (spawning) new Gaussian functions on the PEH of state J. The likelihood of an ISC process is evaluated computing an effective coupling parameter, which is proportional to the ratio between the corresponding SOC and electronic energy gap. If the effective coupling parameters is larger than a predefine threshold, and the resulting new spawned basis functions will have an overlap with the parent basis functions larger than a certain value, then ISC is supposed to happen and the

spawning process on the J PEH is indeed undertaken. In both papers the new approach have been tested using a Breit−Pauli Hamiltonian in order to account for the SOC. In the first of these two papers,[74] resulting from the work of Martinez and co-workers, the new approach, called generalised AIMS (GAIMS, see Figure 4), has been tested on a model system and for simulating the non-adiabatic dynamics of thioformaldehyde. For the model system GAIMS reproduces the exact results within a maximum deviation of 7%. In the characterisation of thioformaldehyde, GAIMS describes a small but sizable population of the T_2 $\pi\pi^*$ state in a 200 fs time window after S_1 $n\pi^*$ excitation. In the second of these two papers,[75] resulting from the work of Varganov and co-workers, the approach was tested studying the ISC process between the excited $^3B_1$ and ground $^1A_1$ states of GeH_2 and comparing the results with values calculated using statistical non-adiabatic transition state theory. From the comparison a shorter $^3B_1$ lifetime is predicted based on the improved version of AIMS, which is ascribed by the authors to the ability of the implemented method to account for ISC processes at any point along the intersection seam. While Martinez and co-workers used in their tests an interface between AIMS and Molpro in order to compute the needed SOCs, Varganov and co-workers created an interface between AIMS and GAMESS.

In 2016 the exact factorisation of the electron-nuclear wave function has been employed for deriving a trajectory-based dynamics method and in 2017 the so derived approach was used for the first time for simulating the photoexcited dynamics of a molecular system.[76, 77] In the exact factorisation the solution of the TDSE is written as a single product of a time-dependent nuclear function and a time-dependent electronic-function, which leads to a decomposition of the original TDSE in coupled equations for the nuclei and the electrons. The nuclear equation is a standard nuclear TDSE, but evolving on a "time-dependent" PEH (TD-PEH) and including a time-dependent vector potential, which can be seen as the time-dependent analogous of the non-adiabatic coupling vectors. In the electronic equation, the presence of a so-called "electron-nuclear coupling operator" couples the evolution of the electrons with the nuclear degrees of freedom. Min, Agostini, and co-workers, formulated a coupled-trajectory mixed quantum-classical (CT-MQC) scheme able to solve the two equations.[76, 77] The approach is based on three main approximations. First, the classical limit of the nuclear equation is derived, and the corresponding Newton equation is instead treated. Second, the time-dependent electronic function is expanded, accordingly to a Born-Huang-like expansion, in the basis of electronic adiabatic states. Third, the term that determines explicit dependence in the electron-nuclear coupling operator on the nuclear wave-function is approximated employing information obtained from the trajectories. The resulting CT-MQC equations simply require quantities that can be obtained by standard electronic structure packages, consequently allowing the on-the-fly implementation of the method. In order to test the CT-MQC performances, and in particularly its intrinsic ability to correctly account for decoherence effects (which is a well-recognised pitfall of TSH methods), the method have been employed for simulating the photochemistry of oxirane in gas phase, comparing the results with simulations obtained using fewest-switches surface hopping (FSSH) and a corrected version of this algorithm (corr-FSSH) that accounts for quantum decoherence in a phenomenological manner. The results show the ability of CT-MQC to correctly describe quantum decoherence without the need for empirical corrections, as in corr-FSSH, and to have with respect to the latter method a better convergence with the number of trajectories. Further work on the use of the exact

factorisation for dynamics simulations performed by Curchod and Agostini analysed the topological features of the TD-PEH and of the time-dependent vector potential.[78] From their study it emerged that both the TD-PEH and the time-dependent vector potential behave at all times as smooth function of the nuclear coordinates, even in the region of CIX. This latter fact is very promising, since it shows that the EF formalism greatly simplifies the description of non-adiabatic processes, even in the presence of CIXs, which in the adiabatic representation lead to the well-known singularity of the non-adiabatic coupling vectors.

In the ML-MCTDH method, the key idea of MCTDH (*i.e.* an efficient expansion of the N dimensional nuclear wave-function in a sum-of-products of functions, called single-particle functions (SPFs), with reduced dimensionality) is in turn re-used in order to expand the SPFs. The resulting SPFs can again go through a time-dependent multiconfiguration expansion, and the procedure can be repeated for each new set of SPFs, creating various "layers" in the original expansion, from which the name "multi-layer" MCTDH arises. As in MCTDH, the last expansion will be on the basis of one-dimensional time-independent functions, called primitives. In each layer of MCTDH expansion, SPFs having a certain dimensionality, are expanded in term of a basis functions (either new SPFs or primitives) having a reduced dimensionality. For example, in a three-layer ML-MCTDH approach, the original wave-function is described by a first MCTDH expansion (first layer), each of the so-resulting SPFs are in turn expanded accordingly to a new MCTDH expansion (second layer), and finally, the SPFs generated by the second MCTDH expansion are expanded in the basis of the time-independent primitives (third layer). The method is known to be very efficient and able to treat systems of hundreds to thousands of degrees of freedom. For example, in 2017, ML-MCTDH has been used for running dynamics in a high-dimensional model of the LH2 antenna complex of purple bacteria.[79] Before a ML-MCTDH dynamics can start, a specific multi-layer structure must be chosen, answering the following three questions. How many times the SPFs are expended accordingly to a new MCTDH expansion? How many SPFs are used in each expansion (which in turn determines the number of configurations in each expansion)? How to combine the degrees of freedom (which in turn determines the reduction in dimensionality undertaken in each layer)? These decisions are key for the efficiency of the methods, and are normally taken on the bases of prior experience and a "trial and error" approach. In 2017, Mendive-Tapia and Gatti proposed a more systematic way for both selecting the number of SPFs and combining the DOFs, implemented in the so-called ML-spawning algorithm.[80] The central idea behind their implementation is to start with a reduced number of SPFs, and then automatically increases their number during the dynamics in a "on-the-fly" fashion, using as a criteria the value of the lowest natural orbital population. The natural orbital population of each SPF is in fact related to the importance of the corresponding SPF for the wave-function. Normally, in a considered converged dynamics, the value of the lowest natural orbital population should not be greater than 10^{-3}. In the ML-spawning approach when the value of the lowest natural orbital population is above a predefined threshold, more SPFs are created (spawned) into the dynamics. The method consequently follows the philosophy or adding new resources (in this case SPFs) when the dynamics requires them, consequently saving the effort of starting with too many resources (SPFs) than needed, which is particularly true at the beginning of a dynamics where a wave-packet is normally quite localised and fewer SPFs are enough. Regarding the way of

combining DOFs, the authors suggested that DOFs that in a ML-spawning simulations grown (*i.e.* rate at which the associated SPFs are increased) in a similar fashion, should be grouped together. This idea, although successful for the tested cases, implies that test dynamics must be run in order to identify the most efficient way of combining DOFs. The ML-spawning method was tested running simulations on the non-adiabatic dynamics of pyrazine from the S_2 excited state and on the quantum dissipative dynamics in a spin boson bath, showing for both cases a significant computational saving using the ML-spawning approach with respect to normal ML-MCTDH implementation.

Apart from the above reported contributions on quantum dynamics, which provided just a selection by no means meant to be exhaustive, various significant contributions have been presented for semiclassical dynamics. Here we just mention the publication of two thorough reviews on the famous surface hopping method, one presented by Subotnik *et al.*,[81] the second published by Wang, Akimov, and Prezhdo.[82]

3 Conical intersections and their role in photophysics and photochemistry

CIXs are quantum-chemical entities that arise from the Born-Oppenheimer approximation of the Schrödinger equation as regions of crossing between at least two PEHs. In case of involving singlet electronic states, they are simply called CIXs, while for crossings between singlet and triplet spin-free states, the term STC is commonly used. As mentioned in the Introduction, they represent the non-adiabatic processes IC and ISC, respectively, and are related to ultrafast excited-state chemistry, in the first case, and spin multiplicity changes, in the second case. In order to properly describe these PEH crossings, special quantum-chemistry methods are needed able to describe at the same time at least two electronic configurations (representing each one of the electronic states which cross). For example, the E/Z photo-isomerisation of ethylene is characterised by a CIX that is reached by elongating the double bond, twisting it and pyramidalising one of the carbon atoms. At such crossing structure, two electronic configurations (diradical and zwitterionic) become energetically close. Methods using only one configuration (single-reference methods) cannot deal with the multiconfigurational nature of these crossing regions, multi-reference methods being the most appropriate to provide with an accurate description. One of the most general and practical methods is CASPT2, which has a good accuracy in photo-chemistry and excited-state chemistry for small and medium-size molecules. Such usefulness is evident in the bibliography analysis done in this work (it is the most used method in CIX studies; see Figure 5a). Other methodological strategies are also already available which were developed to allow approximate solutions in the CIX region. They are motivated by the fact that CASPT2 computations are relatively slower as compared to other types of methods such as TD-DFT and become prohibitive for practical applications in large-size molecular systems or semi-classical dynamics studies with a large ensemble of trajectories. It is however not always possible due to the intrinsic multiconfigurational nature of the CIX. Regarding computational strategies, it is worth noting in Figure 5b that a significant percentage of articles have addressed the determination of time-dependent properties by using either a quantum or semiclassical approaches. Whereas in the former, a quantum description is provided for both electrons and nuclei, in the latter, nuclei positions and velocities are

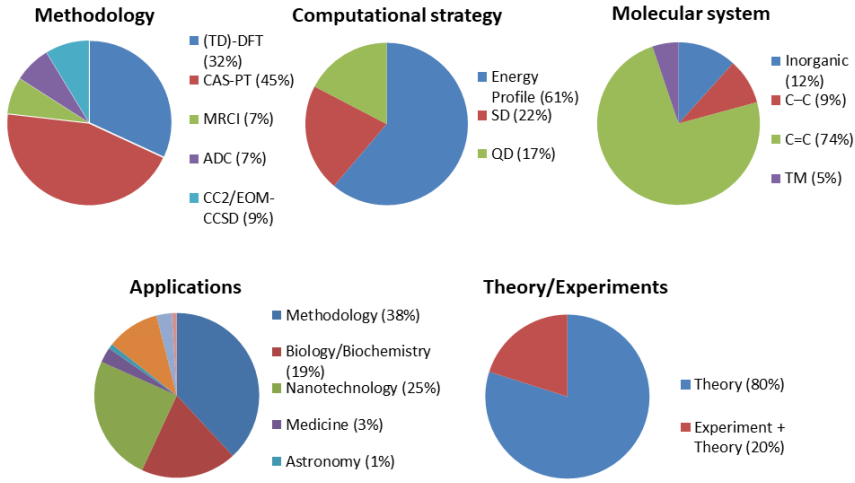

Figure 5. Statistics calculated on the basis of CIX studies published in 2016 and 2017. Distinct concepts are analysed: the method used to PEHs at or around the crossing region (a), the computational strategy to obtain the excited-state chemistry (energy profiles or semiclassical/quantum dynamics) (b), the chemical nature of the studied molecules (c), the main fields of application (d) and the type of work (e) (201 articles considered).[83]

obtained by integrating Newton's equations and using electrons gradient computed with quantum methods. As can be seen in Figure 5, non-adiabatic chemistry or CIXs have been mainly studied in organic π-conjugated molecules (Figure 5c, C=C) with relevant implications for the design of new materials in nanotechnology or to understand the mechanisms present in nature derived from light-matter interaction (Figure 5d). Note also the large percentage of studies focused on improvements of methodology to more accurately treat CIX or to decipher new conceptual or mechanistic aspects of the PEH crossings (Figure 5e). Finally, it is interesting to see that there is a significant number of studies in which CIX characterisations are carried out together with experimental measurements.

In this work, in order to illustrate the relevance of CIXs and the synergy of joint experimental-theoretical research approaches, we shall review a few works carried out by some of the authors of the present chapter mainly during the period 2016-2017 and focusing on the characterisation of the CIXs and their link to observable data in the experiments. In particular, we shall focus firstly on the CIX which are reached upon an excited-state double-bond E/Z isomerisation[84,85,86] and secondly, those which imply twisting of bonds in composites of borane clusters and organic rings.[87,88,89,90] As we shall see, CIXs are useful depending on the case for the design of molecular rotors, organic photovoltaics and better luminescent materials.

In 2016, we performed a joint experimental and theoretical study on the photochemical properties of indan-1-ylidene malononitrile (IM) and fluoren-9-ylidene malononitrile (FM).[85] They are molecules containing fulvene, which is an interesting chemical structure in the fields of molecular rotors and optoelectronics due to its synthetic versatility, commercial availability and ease of purification for

electro-optic studies. Low band-gap materials can be formed when it is attached to tetrathiafulvene. The experimental study produced ground-state absorption spectra of IM and FM with band maxima at ~350 nm and very short excited-state decay lifetimes in the ps scale for IM and in the order of 100 ps for FM. Systematic computations were performed for the IM, FM and their basic chemical unit, the 1,1-dicyanoethylene (DCE) using the CASPT2 method and computational strategies for determining the photochemical decay paths. The main excited-state properties obtained for these systems were the following:

- *Loss of π-bonding character.* The low-lying excited states mainly implies excitations from orbitals with π-bonding character of the non-cyclic double bond to others with π*-anti-bonding nature. Excited states in IM and FM have CT nature from the cyano moiety to the rings.
- *Elongation, twisting and pyramidalisation.* The minimum energy path in DCE is characterised by the elongation and torsion of the non-cyclic double bond and the pyramidalisation of the carbon atom close to the cyano groups. Such distortions bring the ground and excited-state PEHs energetically close (CIX). As for ethylene, the electronic configuration that represents the two states which cross have diradical and zwitterionic nature.
- *Stabilisation of charge separation upon increasing π-conjugation.* The positive charge density in the rings is more stabilised in FM than in IM. This effect is lower at the CIX. Thus, whereas in DCE the CIX energy is clearly lower than the energy of the excited-states at the Franck-Condon (FC) region, the relative energy decreases in IM and the CIX becomes much less accessible in FM.

The joint experimental and theoretical study[85] allows to interpret the experimental observations. Thus, the lower accessibility to the CIX upon excitation to the lowest-lying excited states found for FM as compared to the findings obtained for IM, which can be associated to the higher experimental decay lifetime of the former. Based on the outcomes, one would suggest DCE/IM excited-state properties for the design of molecular rotors (accessible E/Z isomerisation CIX), whereas those of FM or larger π-conjugated systems (with less-accessible CIX) would be more important for generating optoelectronics materials in which charge separation is an important target.

The elongated-twisted-pyramidalised CIX was also determined in a previous study on indoline, which is the donor moiety of the dye in dye-sensitised solar cells (DSSCs).[84] In such study, which was already reviewed in our previous contribution,[4] the non-radiative decay path via the ethylene-like CIX was associated to the loss of efficiency of the solar cells based on the indoline-dye. We also suggested avoiding flexible double bonds to improve the efficiency. In the same context of E/Z photo-isomerisations, we have recently finished another study in collaboration with the experimental group of J. Gierschner in which we have proposed an interpretation for the distinct luminescence properties of dicyano-substituted π-conjugated materials.[86] Two groups of molecules were considered depending on the relative α and β position of the cyano groups in the non-cyclic double bonds with respect to the central ring of the distyrylbenzene skeleton (α- and β-DCS series, respectively). In chloroform solution, a-DCS molecules were found to have much lower experimental fluorescence quantum yields than b-DCS systems. Meanwhile, in highly viscous/solid solutions and in crystalline state, all quantum yields are clearly increasing. A rough approximation of the non-radiative photochemical path by

performing TD-DFT and CASSCF computations on representative molecules of the α- and β-DCS series showed that whereas the CIX point appears at similar energies for both type of molecules, the vertical absorption energy is higher for α-DCS than for β-DCS and the energy barrier to reach the CIX point is estimated to be higher for the latter compounds. This implies that in chloroform solution the non-radiative decay path is much less probable in β-DCS than in α-DCS, which directly relates to the higher fluorescence quantum yield of the former. A second interpretation of the experimental data that was provided on the basis of the theoretical results was that the higher yields observed in solid solution and crystalline state (which was called solid-state luminescence enhancement) can be related to the large geometrical distortion that is needed to reach the CIX point. Such distortion is largely hindered when the molecules are packed in the solid state, thus favouring the radiative (fluorescence) decay path.

The link between the restricted accessibility to CIX and the luminescence enhancement is also illustrated in a series of studies performed on borane clusters and composites between borane clusters and organic molecules.[87,88,89,90] As it is commonly known, boron hydrides form clusters such as closo, nido or arachno. Meanwhile, they combine to give rise to macrostructures such as the syn-$B_{18}H_{22}$ and anti-$B_{18}H_{22}$ molecules. In 2012, a joint study lead by the theoreticians J. M. Oliva and L. Serrano-Andrés and the experimentalist M. Londesborough explained why the anti-isomer is fluorescent and not syn-$B_{18}H_{22}$.[87] Such explanation was provided based on CASPT2 and photochemical path computations, which showed that the route on the excited state from the FC region to the CIX is barrierless in the syn isomer and has a well-defined minimum in the anti-$B_{18}H_{22}$ molecule. In a subsequent study, the theoretical work predicted that -SH substituents at the 4 and 4' positions of the anti-isomer would give rise to phosphorescence, which was non-significant in the parent molecule.[88] In fact, while triplet population can be only reached in anti-$B_{18}H_{22}$ at the CIX region, which requires to surmount a relatively high energy barrier, the lowest-lying singlet and triplet states are energetically degenerated along the photochemical decay path of 4,4'-(SH_2)-anti-$B_{18}H_{22}$ on the singlet manifold. Therefore, radiative decay from both singlet and triplet states was predicted from the theoretical predictions, which was confirmed by performing the pertinent experiments. In the period 2016-2017, some of the authors of the present book chapter have extended the analyses of borane photochemistry to inorganic-organic composites, particularly, the $B_{18}H_{20}$-(NC_5H_5)$_2$ molecule, which has pyridine (Py) substituents at the 6' and 9' positions of the anti-$B_{18}H_{20}$ system.[89] Experiments show that there is a blue shift of the emission band maximum when measurements are carried out in solution with less polar solvents. The blue shifting continues when measuring spectrum in the crystal and especially at low temperatures. Meanwhile, the lowest and highest fluorescence quantum yield was obtained in solution with high-polar solvents and in the crystal at low temperature, respectively. Theoretical analyses of the rotation of the pyridine rings show small effects on the ground- and excited states energy profiles. Further photochemical analyses indicated that there are two types of excited-state minima, one in which the two organic rings are co-planar and other minima in which they are twisted. According to the CASPT2 results, the former has larger vertical emission energies than the latter. Therefore, the coplanar geometry was associated with the emissive states in the experimental conditions in which blue shifting was observed. Indeed, twisted structures are hindered in solid state. Twisted structures have also larger dipole moments and

accordingly they are expected to be more stabilised in polar solvents. This is in agreement with the band maxima observed in such conditions, which appears red shifted as compared to the other spectra (in solution with less polar solvents or in the crystalline state). Interestingly, the CIX related to the non-radiative decay path in these systems was determined to have a distorted geometry, which implies a rotation and flapping motion of the two pyridine rings. To reach such crossing point, the boron-boron connectivity holding the B(6) atom to the reminder of the boron cluster must be broken. The CIX was found to be energetically above the position of the coplanar and twisted minima and slightly above the position of the bright states at the FC region in the computations *in vacuo*, which are expected to be a good approximation for the experimental conditions in solution with solvents of low polarity. The high dipole moment obtained for the CIX structure indicates that the non-radiative path should be expected to be more accessible in solution with polar solvents and therefore it was associated to the decrease of the fluorescence quantum yield measured in the experiments in such conditions. Finally, the further increase of the yield in the solid state and especially at low temperature was ascribed to the restricted access to the highly distorted structure of the CIX. This is similar to the previous findings for the DCS compounds[86] and points to the crucial role of the CIX to interpret the well-known phenomena of solid-state enhanced luminescence (also known in the literature with the less concrete statements J-aggregation, aggregation-induced emission or aggregation-induced enhanced emission).

Recently, we have also characterised and interpreted the spectroscopic properties of other inorganic-organic composites which are formed when mixing anti-$B_{18}H_{20}$ and pyridine, $B_{18}H_{20}$-8'-Py and $B_{16}H_{18}$-3',8'-Py_2.[90] Both molecules have accessible CIXs on the excited state and accordingly they are not fluorescent. Computations on the former show a STC region along the decay path on the singlet manifold, which could be related to the fact that this system possesses measurable phosphorescence quantum yield of 0.01.

4 DNA/RNA spectroscopy and photochemistry

Understanding nucleic acids' excited states represents a crucial task for modern science since it enhances our comprehension of life evolution and functioning. Processes of utmost relevance, such as the natural selection of the DNA/RNA current chemical structures and the formation of photolesions that may induce serious diseases like skin cancer, have a molecular basis that may be elucidated using the adequate computational tools. However, the inherent difficulties coming from the correct description of the electronic states and their dynamics, the assessment of the influence of the environment and the multi-chromophoric character of DNA/RNA systems, challenge state-of-the-art theoretical methodologies. The development of novel theoretical approaches and the gradual increase in computational power over time allows tackling these major issues and subsequently yielding remarkable advances in the field of DNA/RNA spectroscopy and photochemistry.

The present section covers some of the achievements related to the field reported in 2016 and 2017. It is divided in two subsections. The first one concerns the advances in the comprehension of DNA/RNA spectroscopic features, mainly vertical absorptions and the study of electronic excited-state wave functions, and the second one is devoted to the photochemical pathways that drive the excited-state decay.

Photochemical channels of photostability, damage and repair involving π-stacked DNA/RNA nucleobases will be emphasised as hot topics of research.

4.1 DNA/RNA light absorption

UV light absorption enables the population the excited states of DNA/RNA systems and takes place in nucleobases given its π-conjugated nature. The correct determination of the electronic-state energies and the relative positions of the bright (or optically active/allowed) states is fundamental because it determines the initially accessed electronic state upon light absorption and allows direct comparison between theoretical and experimental data.

Single nucleobases and related structures. Recent efforts have been dedicated to assess the specific impact of the environment in the excited-states calculation of DNA/RNA monomeric nucleobases. The absorption spectrum of DNA/RNA nucleobases can be simulated sampling the FC region to obtain a set of nuclear coordinates, which are later on used to compute the vertical absorptions on top of each geometry.[91] Pola *et al*[92] have used a Wigner distribution (quantum harmonic oscillator) on the FC regions of the four DNA nucleobases to assess the impact of the first solvation shell, explicitly included in the system. The authors show non-negligible solvent effects, demonstrating the well-known destabilisation on the n,π* states due to the explicit hydrogen bonding of water.

Another usual approach to include environmental effects is the so-called quantum mechanics/molecular mechanics (QM/MM) hybrid approach, in which the chromophore(s) is(are) described with accurate quantum mechanics (QM) methods whereas the environment is treated as point charges surrounding the QM part. Within this approach, the FC region can be sampled by means of MD or QM/MM MD simulations. Martínez-Fernández *et al* [93] have recently validated this methodology to correctly capture the blue shift in the absorption spectrum of 5-methylcytidine due to solvent effects. The authors have employed three different solvation approaches and have contrasted the theoretical results with experimental recordings. Nørby *et al* [94] have reported averaged embedding parameters for nucleobases inserted in DNA double strands, with the aim to save computational time without a significant accuracy loss when making use of the polarizable embedding model to compute DNA optical properties. The proposed approach was illustrated with 2-aminopurine, a common DNA probe, as a model compound. The authors showed that treating the bulk water around the DNA double strand as a continuum has slight impact in the UV spectra as compared to reference values.

Nucleobase clusters. The comprehension of the spectroscopic properties of nucleobase monomers constitutes a first necessary step towards understanding DNA/RNA photochemistry. Nucleic acids are however polymeric chains of chromophores and therefore absorption studies must be expanded to nucleobase multimers in order to describe additional phenomena such as delocalised excitons and charge/energy transport taking place all over the double strands.[95] Nevertheless, the complexity for describing the absorption properties of nucleobase clusters, interacting either via Watson-Crick (WC) base pairing and/or π-stacking interactions, increases with the number of atoms considered, requiring larger computational efforts. Nogueira *et al*[96] have performed a QM/MM study of a solvated polyadenine

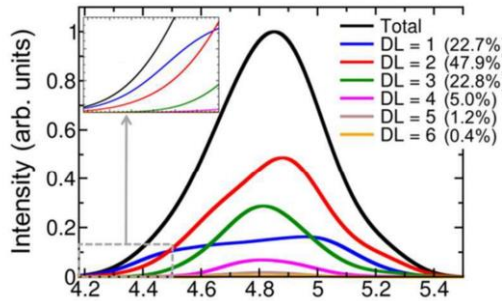

Figure 6. Decomposition of the lowest-energy band of the UV absorption spectrum of $(dA)_{20}$ computed using the QM/MM approach and the TD-DFT method on top of 100 different geometries. DL stands for delocalisation length, followed by the number of stacked adenine molecules. [Reproduced from *Chem. Sci.*, 2017, **8**, 5682 with permission from the Royal Society of Chemistry].

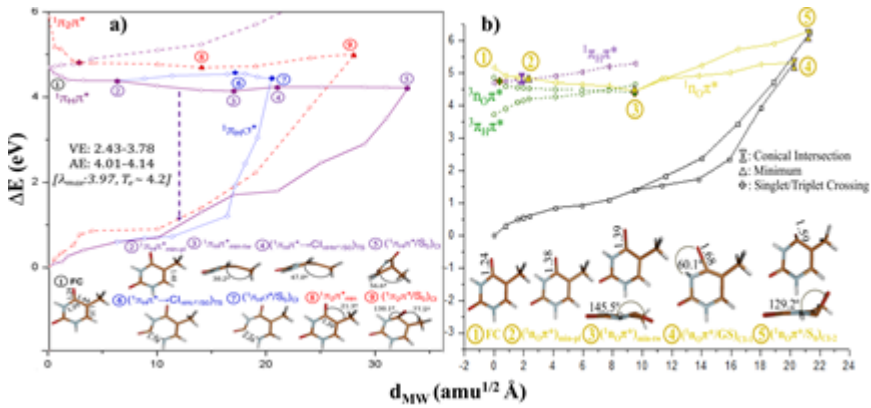

Figure 7. Evolution of the different lowest-lying electronic excited states for water-solvated deoxy-thymidine. Panel a displays the ultrafast decay channels, based on $^1\pi\pi^*$ ($^1\pi_H\pi^*$ in purple and $^1\pi_2\pi^*$ in red) and $^1\pi_H\sigma^*$ excitations depicted in blue, whereas panel b shows the longer-lived channels featuring optically dark $^1n_O\pi^*$ state in yellow and two different triplet ($^3n_O\pi^*/^3\pi\pi^*$) states in green. Panel a is reproduced from *J. Phys. Chem. Lett.*, 2017, **8**, 1777 with permission from the American Chemical Society. Panel b is reproduced from *Phys. Chem. Chem. Phys.*, 2018, **20**, 6877 with permission from the Royal Society of Chemistry.

$(dA)_{20}$ double strand determining the excited states of eight π-stacked adenine nucleobases making use of a TD-DFT method to describe the electronic states. The quantitative analysis of the delocalisation extent of the excited-state wave functions, shown in Figure 6, revealed that light absorption takes place mainly over two adjacent nucleobases (47.9%), whereas excitations localised over monomers (22.7%) and trimers (22.8%) also contribute to the spectral intensity. Another important conclusion of the work is that the observed hypochromism in DNA can be mainly explained by long-range interaction between nucleobases, and not by delocalisation or charge-transfer phenomena. The remarkable delocalisation over the stacked adenine moieties was also reported by other computational studies using coupled-

cluster methods.[97, 98] In particular, Sun *et al*[98] used *ab initio* results to parameterise DFT functionals to describe the excited states of a series of DNA tetramers, including alternating and non-alternating AT and GC oligomers. Results also showed vertical delocalisations between π-stacked nucleobases not only for AT but also for GC dimers. By using a different approach, Saha and Quiney[99] applied the effective fragment potential method[100] to represent the solvent effects in model AT dimers, showing that hydration enhances delocalisation in π-stacked AT clusters whereas showing much less delocalisation in the WC arrangement. The authors interpret this phenomenon in light of the number of hydrogen bonding with the solvent available for each model system.

4.2 DNA/RNA decay pathways

The natural photostability of nucleic acids, survivors in a world flooded by UV radiation, has been ascribed to the intrinsic ultrafast decays displayed by natural nucleobases.[101] From a theoretical standpoint, this fact has been often explained due to the barrierless decay of the π,π* bright state towards the CI with the ground state in an ultrafast (sub-ps) manner.[95, 102] Even though this phenomenon is fairly well understood, there are still some open questions without a satisfactory answer, such as the excited-state mechanism of non-canonical nucleobases or the deactivation routes responsible for the long-lived (several to dozens of ps) excited-state components recorded experimentally in double-stranded DNA/RNA.[95]

Decay pathways of nucleobase monomers and related structures. The advent of new developments as those previously outlined in Section 2 has paved the way for the use of more correlated methods in the characterisation of the photoinduced phenomena triggered in DNA/RNA nucleobases and nucleosides upon UV-light irradiation. Recent studies have shown the intrinsic differences obtained by mapping the different PEHs of nucleobases[103] and nucleosides,[104, 105] at the CASSCF and CASPT2 levels of theory, illustrating how dynamic correlation is key to faithfully depict photoinduced phenomena in these species (see Figure 7 for the particular example of deoxy-thymidine). Despite displaying similar PEHs as those reported at the CASSCF level,[106] MS-CASPT2 results highlight the role of dynamic correlation in enhancing the ring puckering motion along the main reaction coordinate as shown by the characterised $^1\pi_H\pi^*$ twisted minimum (see Figure 7a) not featured at CASSCF. Moreover, dynamic correlation also plays a key role in stabilising the $^1\pi_H\sigma^*$ state, which under solvation offers an alternative competitive decay channel through a ring-opening CIX with the ground state. Figure 7b shows the dark states ($^{1/3}n_O\pi^*$ and $^3\pi\pi^*$), which display a lesser dependence to dynamic correlation and thus resemble more those previously obtained at the CASSCF level.[107] The PEHs and associated spectroscopic signals have been shown to be in agreement with the available experimental evidence, not just for canonical nucleobases but also for epigenetic modifications such as 5-methyl-cytosine,[108] which display an increased lifetime with respect to its canonical form.

Decay pathways of nucleobase clusters. The presence of additional nucleobases in photoexcited DNA/RNA oligonucleotides opens alternative decay routes to the monomeric decays localised in a single nucleobase, due to π-stacking interactions and the WC hydrogen bonding occurring in DNA/RNA double strands. Whereas the

former interactions are usually ascribed to long excited-state lifetimes[109, 110, 111, 112, 113] and the formation of photolesions such as cyclobutane-pyridine dimers (CPDs) or 6-4 adducts, the inter-strand hydrogen bonding drives photoresponses at the picosecond scale, as shown by recent experimental measurements.[114, 115, 116]

The disentanglement of the excited-state components measured at very different timescales[117] represents a challenge for the scientific community and needs the use of theoretical methodologies to resolve the riddle. Using TD-DFT in combination with continuum models, it has been recently suggested that the nanosecond fluorescence registered experimentally correspond to the presence of high-energy long-lived mixed (HELM) states.[118, 119] These states constitute mixtures of intra-strand Frenkel excitons and CT excitations over alternated AT and GC DNA oligomers. It is proposed that the long-lived fluorescence indeed correspond to the exciplex emission from the excited-state minima of the HELM states. Recently, the decay rate for the electron transfer process from the intra-strand CT state to the ground state in GC stacked dimers has been studied using theoretical methods.[120]

One of the most common photolesions in DNA is the occurrence of excited-state cycloadditions, which covalently bond the π-stacked nucleobases leading to CPD structures that can induce mutagenesis. Rauer *et al* [121] have studied the photodimerisation of π-stacked thymine dimers by means of surface-hopping MD using the CASSCF method. In this study, the photoreaction took place in the single manifold even though ISC processes with triplet states were allowed to occur. The authors reported that the photo-cycloaddition is mediated by a doubly excited state delocalised over two thymine moieties, placed above the bright state at the FC region. It was suggested that the system needs to overcome an energy barrier in order to populate the reactive state. In a different work, Mendieta-Moreno *et al*[122] conducted QM/MM non-adiabatic simulations to study the same photoprocess. The authors reported the presence of energy barriers attributable to the motion restrictions imposed by the WC hydrogen bonding and the sugar-phosphate backbone. Given the significance of the CPD lesions, even though they are formed in low yield, cells need to repair the photodamage in order to preserve the correct biological function of nucleic acids. Photolyases constitute a family of enzymes that are able to repair the damage absorbing blue light. Notwithstanding the relevance of these processes, the molecular basis of the reparation is not completely understood yet. Lee *et al*[123] have applied QM/MM methodologies to study the photorepair processes, reporting a variety of competing charge-transfer states that could explain the high repair yield of the enzyme.

Photodimerisations involving other nucleobases have also been recently studied. The adenine-adenine photoreaction mechanism was tackled by Banyasz *et al*.[124] The authors explained the base-sequence dependence of the experimental quantum yield of the photolesion in terms of molecular-orbital interactions between the two adenine nucleobases. Another study on the adenine-thymine dimerisation also revealed the remarkable influence of the relative *syn*/*anti* orientation between the two nucleobases influencing the reactivity of the photo-cycloaddition.[125]

Another kind of photolesions consists in the formation of a single C-C bond between two adjacent pyrimidine nucleobases, leading to the so-called 6-4 adducts. Recently, the photoprocess taking place between two stacked thymine molecules was studied by Giussani *et al*[126] employing the QM/MM approach, describing the QM part with the CASPT2//CASSCF protocol.[127] The authors found a reactive path along the PEH of a charge-transfer state from the 5-end to the 3-end thymine. From

a pro-reactive initial structure, the CT state can decay towards a CIX with the ground state, from which the system, after surmounting an energy barrier on the ground-state PEH, can lead to the formation of an oxetane ring, the known intermediate for 6-4 adducts production.

Regarding the photochemical decay channels involving the hydrogen bonding between opposed nucleobases, *i.e.* WC base pairs, recent efforts have been devoted to understand the electron-driven proton transfer processes in presence of additional π-stacked nucleobases.[128] It has been recently shown that not only inter-strand CT states can initiate the process but also intra-strand CT states.[129] Martínez-Fernández *et al*[130] have studied the PEHs associated to these types of mechanisms in alternate GCGC and ATAT tetramers, reporting a barrierless profile for the former and the presence of a significant barrier for the latter, in agreement with the available experimental evidences.

Despite recent advances, more sophisticated and better-resolved spectroscopic methods are sought in order to unequivocally assign the different deactivation channels populated in DNA upon UV-exposure. One recent development in that front comes from two-dimensional electronic spectroscopy (2DES), where an enhanced spatial and temporal resolution is obtained with respect to the widely used standard pump-probe set-ups and that has the potential to separate monomeric contributions to those due to excimer/exciplex formation in oligomeric systems. Moreover, this technique is in principle also able to disentangle specific conformations in solvated dimeric and multimeric systems, elucidating the concrete conformations favouring specific channels.[131, 132, 133] The field is still in its infancy and plenty of work has been dedicated theoretically to the accurate description of the seldom studied high-lying excited state manifold, which characterise the different transitions recorded in these complex experiments.[134, 135, 136]

5 Photosensitisation of biological structures and photodynamic therapy

With the notable exception of important chromophores such as retinal embedded in rhodopsin or photosynthetic systems, whose biological significance is obvious, most of the biological polymeric structures, nucleic acids, proteins, and lipid membrane do not absorb visible light, and are instead sensible to ultraviolet UVA and more often UVB and UVC light. This feature can be easily understood in terms of the necessity to protect their integrity in the biological environment, as absorption of light may trigger unwanted photochemical reaction leading to the destruction or modification of the biological structure and hence ultimately to the cell death or to mutation. Actually, given the amount of UVC and UVB light reaching the Earth being filtered by the ozone layer one can recognise a protective strategy of biological organisms to limit the unwanted effects of exposure to the sun as already mentioned in Section 4.2. Direct damage produced by direct exposure, especially in the case of nucleic acids, cannot be neglected, being related to skin cancer (*cf.* Section 4.2). Here, we want to consider the indirect effects produced by relative small chromophores interacting covalently, or most often non-covalently, with biological systems and able to absorb light in the UVA or visible region of the spectrum to subsequently trigger photochemical and photophysical phenomena resulting in the production of damages in the biological structure. The latter is the process known as photosensitisation and from a photophysical and photochemical

point of view one can recognise different types of mechanisms. The most common processes involved in sensitisation are related to ISC, *i.e.* the sensitizers are supposed to populate its triplet manifold with a reasonable efficiency, the triplet states may then evolve to induce electron- or energy-transfer, in a sort of direct mechanisms, or may lead to the production of singlet oxygen ($^1O_2$) that will subsequently produce oxidative lesions to the biological systems. However, we will show in the following that such a characterisation is certainly too simplistic and indeed, several different and competitive pathways, including or not triplet population, should be taken into account to provide a comprehensive picture of the phenomena into play.

Photosensitizers can be of different nature, but in general are constituted of π-conjugated aromatic moieties, and where the presence of relatively heavy atoms, such as sulphur, may increase the ISC efficiency.[137] As an example we remind that polyunsaturated hydrocarbons, produced by fuel combustion and present in the air as a source of pollution may also act as sensitizers, urging to the development of a protective strategy and to the comprehension of the combined pollution plus UV exposome.[138]

Despite the possible harmful effects related to photosensitisation, the former general process is nowadays gaining a very important popularity as the base of the so-called photodynamic, or light assisted therapeutic strategy.[139] The latter are indeed based on the combination of drug administration and exposition to light in order to treat resistant lesions such as surgically untreatable cancers. It is noteworthy that the previous strategy has also been used in antimicrobial and antiviral therapy, as well as in food industry for water and food processing. In many instances, photodynamic therapy requires the use of photosensitizers able to produce $^1O_2$. Furthermore, in order to allow for the non-invasive treatment of deep lesions, sensitizers absorbing in the red or infrared regions of the solar spectrum are strongly envisaged to reach the therapeutic window (650-1350 nm) in which human, and in general biological, tissues are transparent.

From those two examples it appears evident how sensitisation may be considered both as a fundamental process necessary to be understood to rationalise the insurgence of harmful diseases and as an opportunity to develop novel therapeutic strategies and drugs. Hence, it is not surprising that a considerable amount of theoretical work has been devoted to such problems in the past two years. From a computational point of view the task is extremely challenging requiring a very well balanced description of different spatial and temporal scales. Indeed, a fully description of the photophysical and photochemical pathways experienced by the different chromophores should be accompanied by a good sampling of the conformational space defining the interaction with the biological system and, at the same time, the specific effects and the influence of the environment should be properly taken into account.

One of the most paradigmatic photosensitisation processes is certainly DNA photosensitisation and benzophenone as a model system has been the subject of a large number of studies[140] elucidating its binding modes[141] and their main photophysical pathways, *i.e.* triplet-triplet energy transfer to thymine.[142] However, the interest of benzophenone relies in the fact that its interaction with DNA may open the way to a number of competitive pathways. In particular and due to the increased basicity in the n-π* excited states, benzophenone can act by hydrogen abstraction either from nucleobases or from the backbone sugar of DNA, hence

possibly leading to harmful lesions including strand breaks. It has been shown[143] that the possible hydrogen-abstraction pathways strongly depend on the interaction modes. Indeed, when benzophenone is interacting in the DNA minor groove, *i.e.* in the most stable conformation,[144] only the backbone sugar hydrogen can be accessed by the carbonyl oxygen. On the contrary, in the case of the double insertion mode, the backbone is not accessible and instead the hydrogen from the nucleobase should be considered as potentially reactive. The free energy profile and the transition state (TS) of the two reactions, *i.e.* H-abstraction from sugar or from the nucleobase, by the T_1 state of benzophenone have been obtained at DFT and wave-function based levels of theory. Results obtained on the isolated model system have unequivocally pointed towards relatively low activation energy of the order of 9-10 kcal/mol, in the same order of some enzymatic reactions. While those results are coherent with the observation that benzophenone may be used as a photocatalyst, these do not explain why the aforementioned pathways and the related photoproduct are observed only marginally. To resolve such an apparent contradiction it is necessary to turn towards the description of the conformational space spanned by benzophenone interacting with DNA as provided by classical MD trajectory. Indeed, if one considers the distribution of the distance between benzophenone carbonyl oxygen and the DNA reactive hydrogens one finds, coherently between minor groove binding and double insertion, that the probability is peaked at around 5-6 Å and only a very marginal population (less than 10%) is found between distances of 2.0-2.5 Å, *i.e.* only a very minor fraction of benzophenone molecules will be at potentially reactive distances with the DNA components, and hence the energy transfer deactivation channel will be favoured compared to the photochemical hydrogen-abstraction. Hence, in a certain sense this mechanism can be regarded as a sort of self-protection strategy, in which the molecular environment of the macromolecules hampers the reactants encounter and hence strongly diminishes the outcome of the reaction despite the presence of a generally low activation barrier. Apart from its biological significance, this study also provides a clear evidence of the complex interplay and equilibrium between photophysical, electronic and structural effects that should be taken into account in the study of the photosensitisation of biological structures.

The effects of the molecular environment in tuning and in some instance driving the available photophysical channels when interacting with DNA is also exemplified in the case of two dyes, nile red and nile blue, widely used in biological applications and proposed as sensitizers acting by photoinduced electron transfer to guanines. The optical and photophysical properties of the two isolated and solvated dyes have been fully analysed underlying their absorption in the visible part of the spectrum and characterizing the different excited states.[145] More importantly, the reproduction of the absorption and emission spectra has allowed from the one hand to underline the importance of dynamic and vibrational effects in shifting the absorption wavelengths with respect to the one obtained from the ground state equilibrium geometry and on the other hand to validate TD-DFT level of theory against high level CASPT2 results. Furthermore, the reproduction of the absorption spectrum from snapshots obtained from quantum-based Wigner distribution or from classical MD, has also provided an alternative way to refine force field parameters. Subsequently,[146] and by using classical MD the interaction modes of the two dyes with self-complementary DNA double strand constituted of guanine and cytosine bases has allowed to pinpoint two stable modes of interaction for both dyes, namely intercalation and minor groove binding. Snapshots issued from the MD trajectories

have then been used as starting points to analyse at hybrid QM/MM level the behaviour of the different excited states. In particular, we have considered local excited states as compared to the states in which the electron is transferred to orbitals localised on the guanine. In the case of the nile red chromophore, it appears that the CT state involving guanine is always higher in energy compared to the local states, whatever the interaction mode considered; hence electron-transfer sensitisation should be excluded for such system. On the other hand, and quite surprisingly, it appears that in the case of nile blue, while intercalation mode always provides energetically inaccessible CT states, in minor binding mode a state inversion operates and the population of the charge-transfer state become possible, hence sensitisation should be considered as possible. This occurrence can be rationalised taking into account the fact that in minor groove binding nile blue will be residing close to the negatively charged DNA backbone, hence stabilizing a CT state leaving a hole, *i.e.* positive charge, on the chromophore. On the other hand, in intercalation the charge separation process will take place in the hydrophobic DNA core, hence destabilizing the CT state. Remarkably enough the effects of nile blue on DNA have been confirmed by experimental results and have also recently led to the latter being officially declared as a potentially genotoxic compound by the European Commission Agencies.[147]

As evidenced in the case of benzophenone, in addition to the more studied sensitisation phenomena based on electron- or energy-transfer and $^1O_2$ activation, an important consideration has been devoted to the study of alternative photochemical pathways possibly leading to harmful photoproduct and therefore to biological structure disruption. As an example, high level molecular modelling has allowed to pinpoint the molecular basis of the induced photo-toxicity of two widely used non-steroidal anti-inflammatory drugs, ketoprofen and ibuprofen.[148] Once again, the combination of TD-DFT and CASSCF/CASPT2 strategy has allowed unravelling an easy accessible pathway resulting in the case of both drug to homolytic dissociation. Hence, the two drugs upon excitation in the UVA region evolve to the production of two highly reactive radical species in the vicinity of the biological structures. Actually, the photodissociation pathway is characterised by very small activation barrier and can be easily accessible upon excitation. In the case of ibuprofen, photodissociation is the only accessible relaxation channel, while in the case of ketoprofen, an analogous of benzophenone, the former is in competition with ISC. However, one should consider that upon triplet population the activation of $^1O_2$ can be triggered contributing to the increase of phototoxicity and oxidative stress. In addition, while classical molecular mechanics (MM) has pointed to the existence of metastable interaction modes with DNA, basically minor groove binding; by using cellular biology assays it has been proved that the combination of exposure to UVA light and to both drugs results in an increase of cell mortality. Given that ibuprofen is used in topic creams to be applied on the skin, its phototoxicity should be taken into account and sun exposure avoided in the case of topic usage.

Going from the domain of phototoxicity to the one of phototherapy, efforts have been devoted to taking into account two main crucial factors: shifting the absorption maxima to the red portion of the spectrum to cover the therapeutical window, and avoid the activation of singlet oxygen to allow the efficient treatment of solid tumours that produce hypoxidic conditions. One efficient way of inducing absorption red-shift is also related to the use of non-linear two-photon absorption (TPA). Indeed, the advantage of TPA is twofold, it allows dividing by two the

excitation energy required by the chromophore, hence doubling the absorption wavelength. Furthermore, TPA requires the simultaneous absorption of two photons and its efficiency depends to the square of the light source. Thus, it significant only at the laser focal point allowing for a much better spatial resolution especially suitable for the treatment of cerebral lesions. The mechanism of action of a TPA active photodrug, *bmec*, able to significantly decrease viability of cancer cell lines has been fully characterised at molecular level.[149] In particular, thanks to QM/MM calculations it has been proved that *bmec* has an important TPA cross-section reaching hundreds of GM, while it may also interact persistently with DNA strands in both intercalation and minor groove modes as underlined by classical MD simulations. The interaction with DNA does not alter the TPA cross-section and hence the efficiency of the drug activation. Finally, the mechanism of action inducing phototoxicity has been elucidating on both the solvated and DNA interacting *bemc* and related to the spontaneous production of solvated electrons by the first singlet excited state (S_1). Indeed, the energy level of the radical cation plus the solvated electron has been consistently found to be lower than that of the S_1 state. The interaction with DNA does not modify this feature allowing for the opening of this photochemical channel both for minor groove binding and intercalation. Both the solvated electron and the radical cation can further interact with DNA components inducing either base lesions or strand breaks.

In addition to the effects of DNA non-covalent sensitizers, increasing attention has been devoted to the photoinduced effects produced by modified nucleobases, either artificial or derived from DNA lesions.[150, 151] Resolving the remarkable differences in the spectroscopic features between the canonical nucleobases and their thionated analogues, as well as the elucidation of the excited-state decay molecular mechanisms of the latter, have received an important piece of computational effort.[152, 153, 154] Substitution of oxygen by sulphur, a heavier element, increases the SOC and therefore increases the efficiency of ISC processes. Thus, the relative positions of STC along the excited-state PEHs play a key role. It has been recently proven that the excitation energies of thiobases are significantly smaller than that of the natural nucleobases, whereas the S_0/S_1 CIXs are placed at almost the same level.[155] The excited-state gets consequently trapped in minima suppressing the intrinsic photostability of natural DNA nucleobases.

Finally, and in addition to the DNA sensitisation, computational studies in the period 2016-2017 have been devoted to the elucidation of the sensitisation mechanism acting against biological lipid membranes. In particular, it has been shown[156] that the photosensitizer methylene blue is able to interact with a lipid bilayer taken as a model of a biological membrane. Methylene blue mechanism of action being related to an efficient ISC followed by the production of singlet oxygen it is used to generate photo-induce oxidative stress affecting the lipid unsaturations. By classical MD, also using biased methods such as potential of mean force (PMF), it has been shown that methylene blue cannot spontaneously penetrate inside the lipid bilayer, the process requiring to bypass a free energy barrier of around 30 kcal/mol. Further QM/MM CASPT2 calculations on selected MD snapshots have shown that the penetration in the membrane actually decreases the ISC probability, and hence singlet oxygen yield, because it reduce the overlap between singlet and triplet energy levels. Therefore, one should suppose that methylene blue would activate molecular oxygen in the vicinity of the membrane polar heads and the reactive oxygen species would have to diffuse to the centre of the layer to reach the

unsaturation. On the contrary, and using a similar protocol combining MD simulations with QM/MM modelling, it has been shown that the naturally occurring hypericin drug[157] is able to spontaneously penetrate in the hydrophobic core of lipid bilayers, hence its density nicely overlaps with the one of the lipid double bond. Furthermore, the photophysical key parameters such us singlet triplet gap and SOCs are less affected by the presence of the membrane environment. As a consequence, hypericin ISC probability should remain high, moreover, since its position overlaps almost perfectly with the one of the lipid unsaturation, it could produce singlet oxygen in close proximity to its target increasing thereby the phototoxicity.

6 Chemiexcitation

Excited-state chemistry arisen from a chemical reaction by a chemiexcitation process has been also the focus of a number of computational works in 2016-2017. We shall firstly describe in this section those works mainly studying the mechanistic aspects of the chemiexcitation which gives rise to light emission (CL) and next the studies with important relevance for the CL phenomena taking place in living organisms (BL). For further reading on the topic, we highlight here a recent extensive work establishing the current knowledge on the molecular basis of the chemi- and bio-luminescence phenomena.[158]

6.1 Chemiluminescence mechanisms

In the CL phenomena, a thermally activated reactant generates a highly-unstable intermediate that undergoes a non-adiabatic transition to an electronically excited state product. The subsequent transition back from excited to ground state product is accompanied by a release of energy in form of cold light. The simplest discovered models for CL transformations consist in unimolecular decomposition of 1,2-dioxetanes and 1,2-dioxetanones. The mechanism of these four-membered ring peroxides cleavages has been extensively studied in the last decade by both experimental and theoretical means. On the basis of these studies,[159, 160, 161] it is known that the unimolecular decomposition of 1,2-dioxetane and 1,2-dioxetanone occurs via a stepwise biradical mechanism. The two-step biradical decomposition implies that once the O-O bond is cleaved, the system enters a biradical region where four singlet and four triplet states are degenerated. After that, the C-C bond rupture begins, leading to dissociation of the molecule into two separated fragments. As we briefly described in the previous contribution to the Photochemistry Specialist Periodical Reports of the Royal Society of Chemistry,[4] a very interesting aspect of this proposed mechanism is the presence of a so-called “entropic trapping” region, in which the molecule can split the population among the degenerated manifolds. The entropic trapping region has been shown to play a pivotal role on the dissociation. It basically, regulates the outcome by delaying the ground-state decomposition and giving time to the system to get access to the excited states, e.g., S_1 and T_1. Based on several experimental studies, the unimolecular decomposition of 1,2-dioxetane and 1,2-dioxetanone has been shown to lead to the formation of triplet excited carbonyl products with the yield of up to 30%. However, the formation of singlet excited state is quite inefficient and can barely reach 1%. Previous theoretical studies on 1,2-dioxetane[159, 160] and 1,2-dioxetanone[162] are in good agreement with this observation. For instance, the computed MS-CASPT2 activation energy for the decomposition of 1,2-dioxetane is of 22 kcal/mol. In 1,2-dioxetanone,

the larger triplet population was explained by Francés-Monerris *et al.* by means of CASPT2//CASSCF computations.[162] The authors found that two triplet excited states, namely T_1 and T_2, are accessible along the peroxide decomposition path, whereas only one singlet excited state (S_1) is available. However, these studies did not clarify how the entropic trapping region determines the efficiency of the CL, as well as what its role is in regulating the outcome, or what the lifetime in the biradical region is. In the period of 2016-2017, substantial efforts have been invested to address these fundamental questions in understanding CL phenomenon. Among the whole list, we would like to begin our journey by reviewing some of them wherein simulations of the actual dynamics of the molecular system are reported.

In early 2017, Vacher *et al.*[163] revisited the biradical O-O rupture mechanism of the parent 1,2-dioxetane to provide some accurate predictions from molecular basis of the reaction process. By initiating the trajectories at the rate-limiting TS, corresponding to the O-O cleavage, with Wigner distribution, and giving 1 kcal/mol of kinetic energy, the authors propagated the "on-the-fly" dynamics through the biradical region. The authors used a time-step of 10 au (or 0.24 fs). Moreover, the hopping between the close-lying surfaces along the MEP was allowed throughout the simulations, which was missing in the former report by Farahani *et al.*[160] This indicates transitions among any of the four lowest-lying singlet states. The PEHs were probed at the CASSCF level of theory with state-averaging over the four singlet states. On one hand, the results of the ground-state dynamics simulations support a so-called "frustration" before dissociations, postponing the decomposition reaction. They also found a relation between the O-C-C-O dihedral angle and the time spent in the entropic trap. The half lifetime of the biradical region has been reported to be $t_{1/2}$= 58 fs. This is indeed shorter than the previous theoretical study in which ground state dynamics of 1,2-dioxetane was examined (613 fs).[160] However, the difference was justified by different initial conditions used in both articles. On the other hand, the results on singlet excited state dynamics have shown that the longer a trajectory stays in the excited state, the longer it takes to dissociate. Therefore, the singlet excited state even further postpones the dissociation. However, no decomposition was observed along the singlet excited state, supporting the extremely low singlet emission yield (0.0003%) which had been reported by experimentalists. The half lifetime of the biradical region is hence increased to $t_{1/2}$ = 77 fs. It is noteworthy to mention that the ISCs between the singlet and triplet states are neglected in this contribution and thus further dynamics simulations taking into account the triplet states are required to complement the statements and give an insight into the CL decomposition of 1,2-dioxetane.

Later in 2017, Vacher *et al.*[164] performed another theoretical study on substituted 1,2-dioxetanes with various CL quantum yields, which was initially studied experimentally by Baader *et al.*,[165] explaining how the entropic trap determines the efficiency of the CL process. The authors here could successfully rationalise why the excitation yield increases with the degree of methylation wherein four hydrogen atoms of parent 1,2-dioxetane were replaced by methyl groups. This methyl substitution enhances the CL yield from 0.3% (parent 1,2-dioxetane) to 35% (tetramethyl-1,2-dioxetane), see Figure 8. In this contribution, the authors applied the same approach as for the previous study on parent 1,2-dioxetane. The results show that the substitution would increase the spent time in the "trap" due to the increase in the number of degrees of freedom which would subsequently increase the

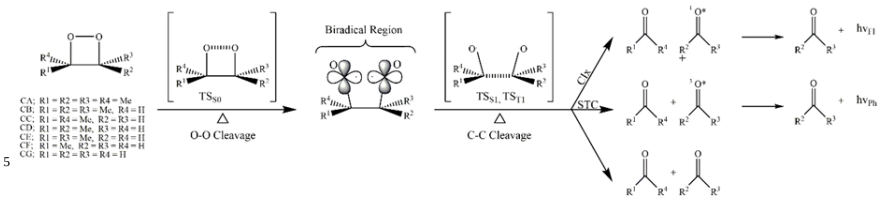

Figure 8. Biradical mechanism has been proposed for the decomposition process of dioxetanes.

population of the product excited state. Nevertheless, the heavier substituents, simply through their larger mass, slow down the torsional motion around the O-C-C-O dihedral angle which can trap the system for longer time and hence postpones the dissociation. Normally, a dihedral angle of 55º is required to escape the entropic trapping region, thus, longer time to reach large dihedral angle equals to slower dissociation. These results are consequently supported by fitting the calculated dissociation half lifetime to the experimental data.

After 1,2-dioxetane, the simplest model for CL and BL transformations is the unimolecular decomposition of 1,2-dioxetanone. To address if there are distinct reaction pathways for the ground and excited state formation in unimolecular four-membered ring peroxide decomposition that possess different activation energies, Farahani *et al.*[166] reported a combined theoretical and experimental mechanistic study on the unimolecular decomposition of *spiro*-adamantyl-1,2-dioxetanone as a prototype. This system was chosen as a model since it is relatively stable and therefore, can be purified by low-temperature recrystallisation. Based on the intensity measurements at different temperatures, the activation energy of the CL is not the same as the activation energy for the decomposition reaction. This indicates the occurrence of two different pathways for the formation of ground and singlet excited state products. To better understand this difference, multiconfigurational approaches with dynamical corrections have been applied to study the unimolecular decomposition. The decomposition mechanism has been shown to be a two-step biradical pathway in which the stationary points are reported to be optimised at the partial CASPT2 level of theory using constrained numerical gradients and composite gradients[167] in conjunction with ANO-L-VDZP basis set. The obtained results confirm the presence of a common TS in the rate-limiting step for ground and excited state product formation. However, the TS corresponding to C-C rupture (not-rate-limiting) is shown to possess different energies for ground and singlet excited states (see Figure 9). It is noteworthy to mention that the theoretical activation energy for the rate-limiting step is overestimated as compared to the experiment. The authors however, justified their results by the deviation involved in the CASPT2 excitation energies using the IPEA correction which was reported in a benchmark study by Zobel *et al.*[168] Nonetheless, they claim that the qualitative aspects of the reaction mechanism is in agreement with the experimental findings.

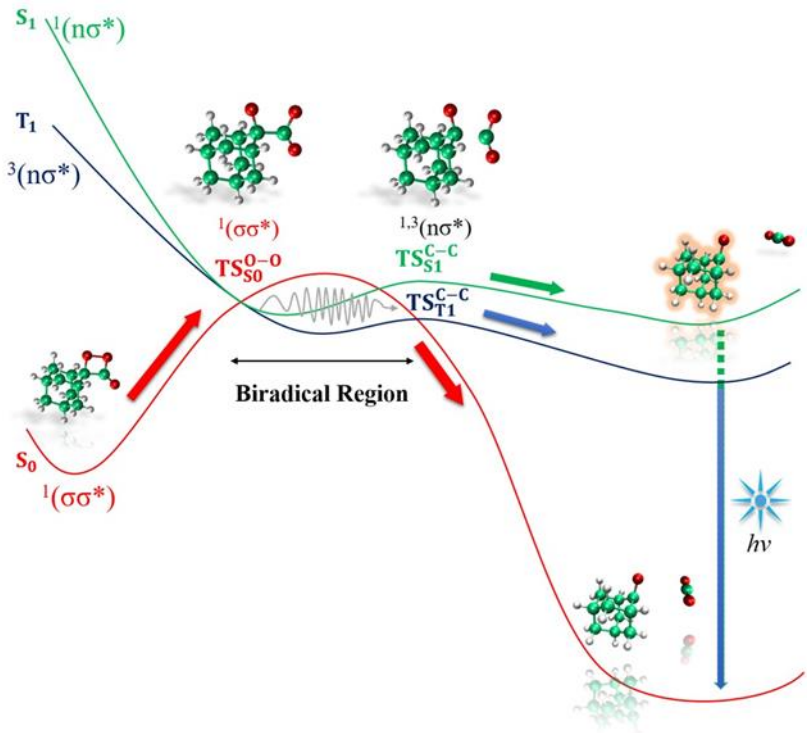

Figure 9. Schematic representation of the PEH for the unimolecular decomposition of *spiro*-adamantyl-1,2-dioxetanone.

In exploring the prototypes in CL reactions, the next generation is 1,2-dioxetanedione. Here, the catalysed decomposition (bimolecular decomposition) is proven to occur with very efficient formation of electronically excited state. This is quite different compared to 1,2-dioxetane and 1,2-dioxetanone decompositions for which the reported quantum yields are shown to be low. To rationalise this difference, Farahani and Baader reported a qualitative and quantitative study on the electronically excited formation of unimolecular decomposition on 1,2-dioxetanedione hoping that it could be applied in the study of bimolecular decomposition of this intermediate. [169] By performing MS-CASPT2 geometry optimisations of the stationary points along the PEH as well as MEP searches, the authors analysed mechanistic aspects of the chemi-excitation process. Interestingly, the findings confirm a concerted mechanism for the ground state dissociation which is contrary to the reported process in 1,2-dioxetane and 1,2-dioxetanone, see Figure 10. The concerted mechanism is a single-step reaction process in which both C-C and O-O ruptures occur simultaneously by overcoming only one TS of 30 kcal/mol. At this TS, the crossings take place which can lead to formation of the excited states. After that, the system enters an extended biradical-like region from which singlet and triplet low-lying manifolds are degenerated. To produce CL, a second TS corresponding to C-C cleavage must be surmounted in the lowest-lying singlet and triplet excited manifolds (37 and 29 kcal/mol for singlet and triplet manifolds, respectively). Since the activation energy for this second TS is higher in singlet

excited state and populating the triplet manifold requires high amount of SOC, there should not be any formation of singlet excited states and/or very low formation of triplet state in the unimolecular decomposition. These findings consequently, support why there is no clear-cut experimental evidence on a direct CL emission from this unimolecular decomposition process.

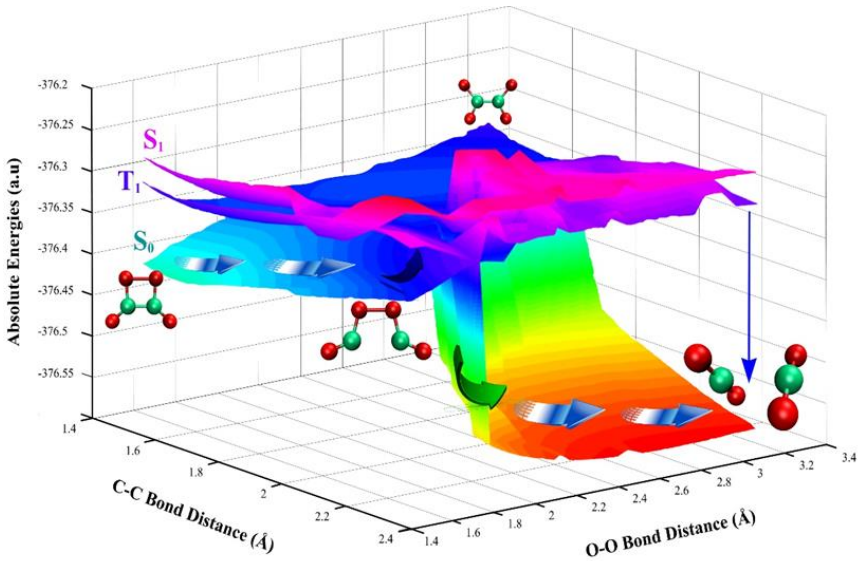

Figure 10. The 2D-PEH of unimolecular decomposition of 1,2-dioxetanedione.

So far, we have only reviewed the studies on unimolecular decomposition of simple models of CL transformation. However, it has been shown that oxidizable fluorescent dyes based on π-conjugated aromatic rings, so-called activators, can promote the decomposition of 1,2-dioxetanones. So that the more the activator is oxidizable, the higher intensity the light emission will have. In 2017, Augusto *et al.* [170] studied on the interactions between unsubstituted 1,2-dioxetane and 1,2-dioxetanone with model activators (naphthalene and anthracene). The CASPT2//SA-CASSCF potential energy curves along the O-O dissociation show an excited-state of CT nature related to the electron-density promotion from the activator to the σ* antibonding orbital of the O-O bond. The energy gap between the ground σσ* and the intermolecular CT excited state πσ* is smaller for the 1,2-dioxetanone complex as compared to the 1,2-dioxetane parent peroxide. This finding supports why activators do not activate the catalysed decomposition of 1,2-dioxetanes and why the efficiency of this process is quite low for 1,2-dioxetanone. The mechanism proposed for the catalysed CL corresponds to two non-adiabatic steps, firstly from the ground σσ* state to the excited πσ* state of CT nature and secondly from the latter to the emissive excited ππ* state of the activator (see Figure 11).

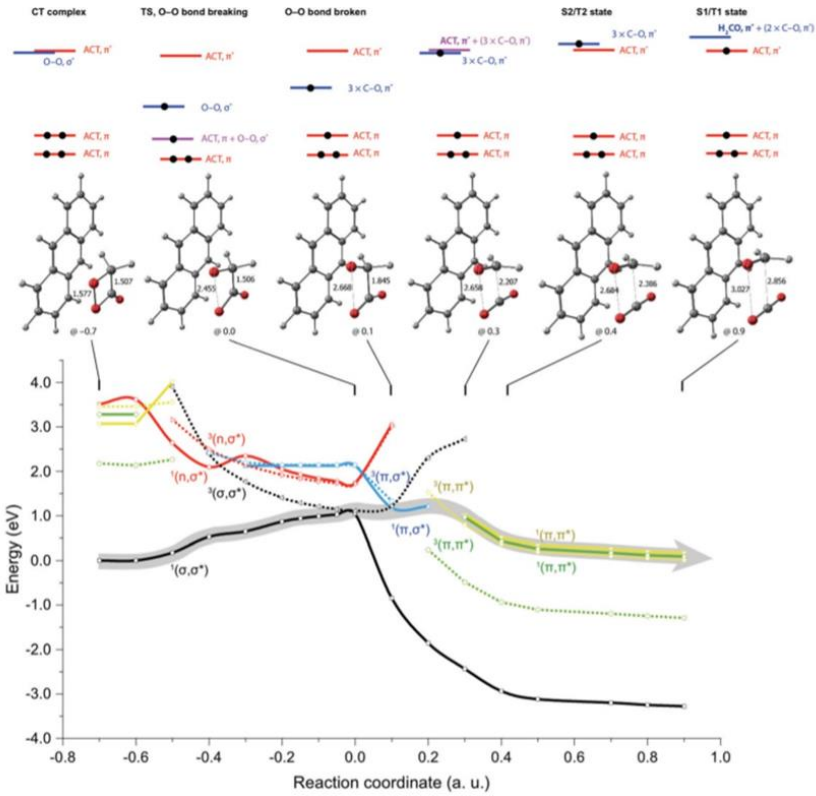

Figure 11. CASPT2//SA-CASSCF PEH for the dissociation of a CT complex formed between parent 1,2-dioxetane and anthracene. [Reproduced from *Phys. Chem. Chem. Phys.*, 2017, **19**, 3955 with permission from the Royal Society of Chemistry.]

6.2 Chemiluminescence in biology: Bioluminescence

BL has been an attractive subject in scientific research for decades due to its broad applications in biotechnology and biomedical fields, such as gene expression, medical imaging, and drug screening. In 2016 and 2017, theoretical studies on BL are concentrated on these issues about the BL mechanism, the chemical structure or protonated species of light emitter, and the factors modulating the colour and intensity of light emission.[171, 172, 173, 174, 175, 176, 177, 178, 179, 180, 181 ,182 ,183 ,184 ,185] The following paragraphs briefly summarised some impressive contributions to firefly,[171, 172] firefly squid,[177] bacteria,[178] and dinoflagellate BL.[180, 181]

Firefly bioluminescence. Among the luminescent organisms, firefly, the well-known BL system, has received the most attention in these two years.[171, 172, 173, 174, 175, 176] These contributions mainly focused on the spectra character and the factors affecting firefly BL. Although the absorption or emission energy of firefly luciferin (LH_2 shown in Figure 12) or its oxidative product (oxyluciferin, $oxLH_2$) have been calculated to be compared to the absorption or emission spectra maximum in experiments, the spectra calculated in the vibrational level was absent. For the first time, the vibrationally resolved absorption and fluorescent spectra of firefly luciferin

were simulated using DFT and convoluted by a Gaussian function with displacement, distortion, and Duschinsky effects in the framework of the Frank-Condon approximation.[171] The firefly luciferin-luciferase system has been applied in the vivo imaging, to investigate the factors affecting light colour and intensity is important. A recent theoretical study employed ONIOM approach to investigate the variation of the barrier heights for the decomposition of the high-energy intermediate of LH_2 (firefly dioxetanone, DO) and its two analogues in the local electrostatic field (LEF) produced by firefly luciferase.[172] The two modified luciferins ($BoLH_2$ and $BtLH_2$) that obviously differ in bioluminescent intensities are shown in Figure 12. $BoLH_2$ and $BtLH_2$ are modified from LH_2 via replacing benzothiazole ring by benzoxazole and benzothiophene ring, respectively. Those calculated results indicated that positive LEF created by luciferase along the long-axis direction (the x direction, see Figure 12) could lower the activation energy and serves as an electrostatic catalyst for DO thermolysis.

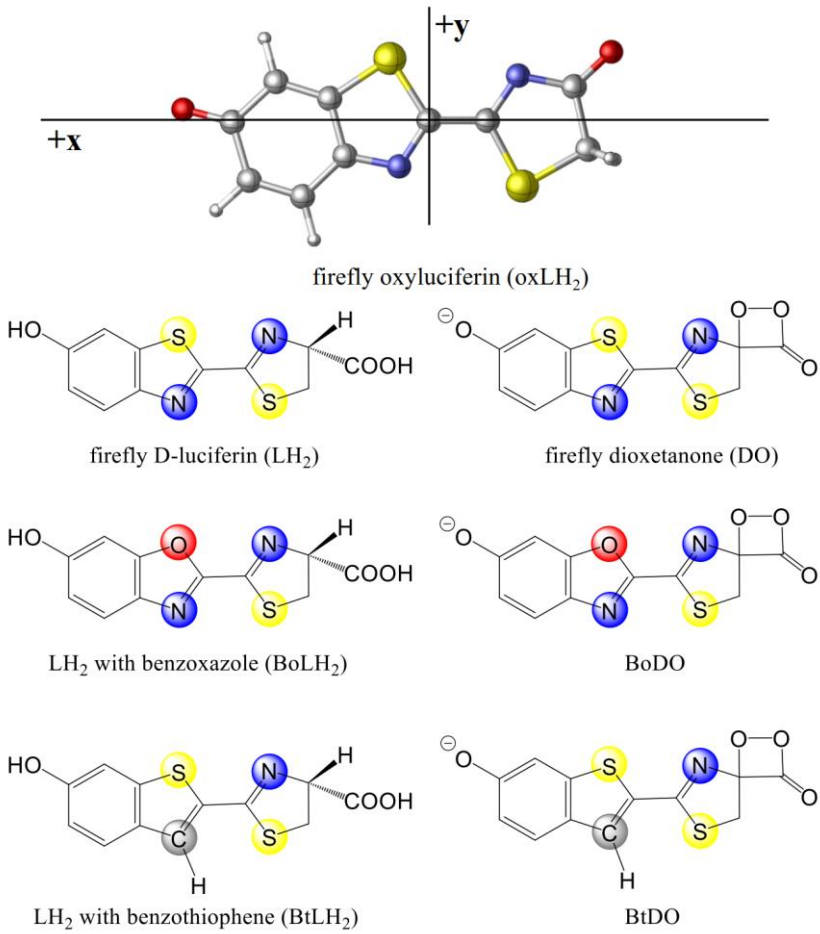

Figure 12. Molecular structures of firefly luciferin and its two analogues ($BoLH_2$, $BtLH_2$: replacing the benzothiazole ring in LH_2 with benzoxazole and benzothiophene, respectively), oxyluciferin ($oxLH_2$) and their corresponding dioxetanones.

Firefly Squid Bioluminescence. Firefly squid luciferin has a universal core structure, imidazopyrazinone (ImPy, the blue skeleton in Figure 13), which is common in the luciferins of about eight phyla of luminescent organisms. But this bioluminescent mechanism remains largely unknown, especially for the two key steps: the addition of molecular oxygen to luciferin and the formation of light emitter. In 2017, the detailed mechanism of the two key steps was investigated for the first time by QM calculation with non-adiabatic MD simulation.[177] By analyzing the energetics, electronic structures, and CT process, the calculated results indicated that (see Figure 13): (1) the oxygenation reaction of luciferin is initiated by a single electron transfer (SET) from the luciferin to molecular oxygen, which occurs at the C_2 position of the ImPy ring in the luciferin. The high-energy dioxetanone intermediate is formed via a nucleophilic addition reaction followed by biradical annihilation and an ISC in the vicinity of singlet/triplet surface intersection. (2) The light emitter is produced from the anionic dioxetanone intermediate via the mechanism of gradually reversible charge-transfer-induced luminescence (GRCTIL) with a high quantum yield Φ_S = 43%.

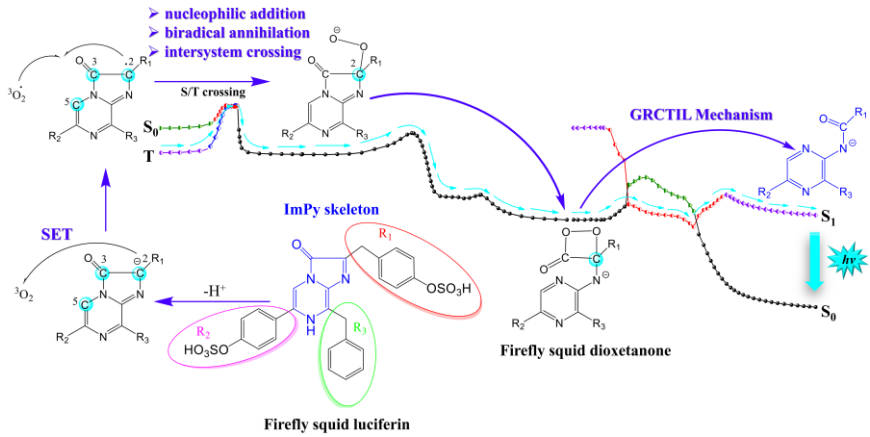

Figure 13. The detailed process for the oxygenation of luciferin and the formation of light emitter.

Bacteria Bioluminescence. Luminous bacteria emit continuous glow and have been widely used in BL imaging fields, especially as a sensitive and convenient tool for monitoring environmental toxin. But the light emitter of bacteria BL is still a debatable point. An intermediate called flavin mononucleotide (HFOH, see Figure 14) and the final products (Flavin mononucleotide, FMN) are assumed as candidates responsible for bacteria BL, because they have similar molecular structures and fluorescence wavelengths. It is worth noting that the similar HFOH and FMN perform opposite fluorescence behaviours in solution and in luciferase. FMN emanates fluorescence in solution but exhibits fluorescence quenching in the bacterial luciferase. What is the exact chemical form of bacterial bioluminophore and why FMN fluorescence quenching occurs in the bacterial luciferase? In 2016, the above problems were solved via high-level QM method, the combined QM and MM method QM/MM, and MD simulation.[178] The calculated results revealed that: (1) the S_1-state HFOH is the bacterial bioluminophore; (2) FMN fluorescence

quenching results from the electron transfer from the quencher (the tyrosine residue 110 in the bacterial luciferase) to FMN with the aid of protein fluctuation.

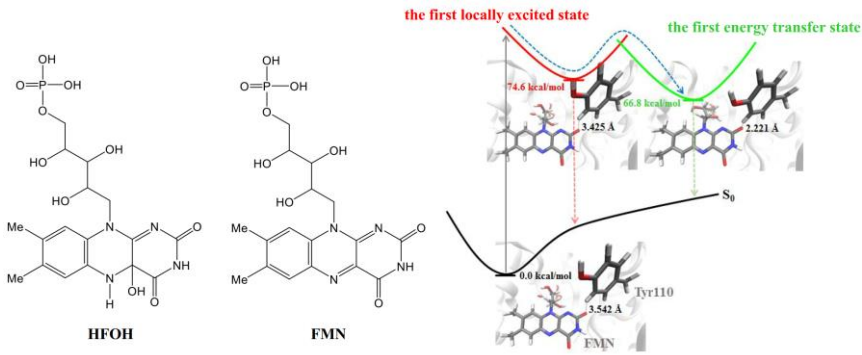

Figure 14. Molecular structures of HFOH and FMN, and the fluorescence quenching process of FMN.

Dinoflagellate Bioluminescence.[180,181] Dinoflagellates BL are featured in two aspects: they are the major component of sparkling lights in coastal water; the sparkling luminescence results from fluid shear stress. This luminescence reaction is a luciferin-luciferase one in which the dinoflagellate luciferin is oxidised to the oxyluciferin with the light emission. (see Figure 15) Generally, the oxyluciferin is the chemical source of light emitter for the luciferin-luciferase systems, such as firefly, *Cypridina*. But dinoflagellate oxyluciferin is not fluorescent. It is not clear that what is the light emitter of dinoflagellate BL and what is the chemical process of light emission. In 2016, dinoflagellate BL is theoretically studied by TD-DFT method for the first time. In this study, the excited-state *E/Z*-isomer luciferin or its analogue rather than oxyluciferin is assumed as the bioluminophore and a Dexter energy transfer mechanism for light emission iss proposed.[180] The excited-state oxyluciferin produced from the oxidation of luciferin acts an energy provider transferring energy to another ground luciferin or its analogue that emits radiative transition. The subsequent theoretical study investigated four chemical forms of intermediate in the luciferase catalytic cycle and suggested that the gem-diol(ate) intermediate shown as Figure 16 is the bioluminophore and *E/Z*-isomer luciferin proceeds via chemically initiated electron-exchange luminescence (CIEEL)/twisted intramolecular charge transfer (TICT) to produce the bioluminophore.[181]

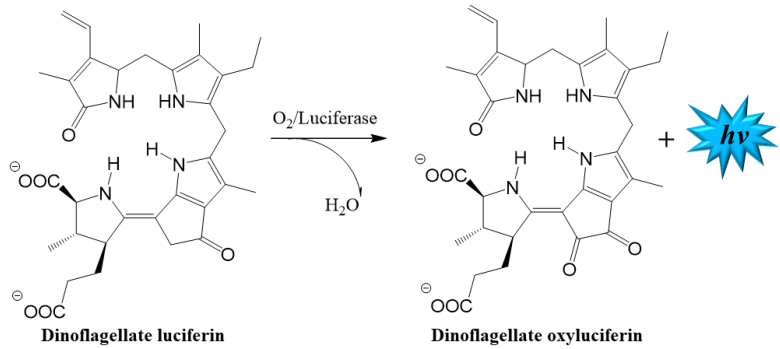

Figure 15. The general process of dinoflagellate BL.

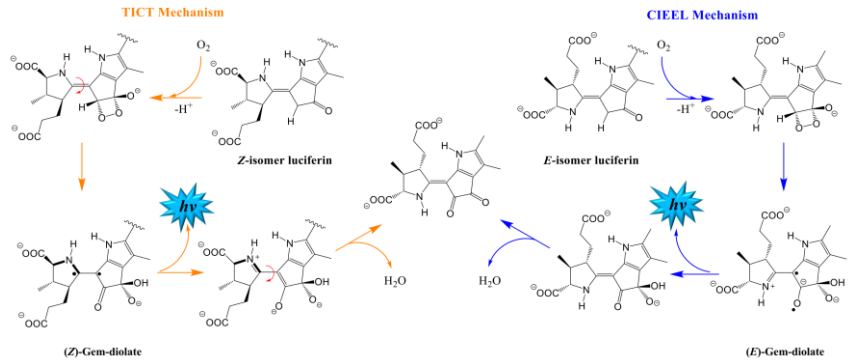

Figure 16. Proposed mechanism of dinoflagellate luciferase catalytic cycle involving CIEEL for *E*-isomer luciferin and TICT for *Z*-isomer of luciferin.

8 Summary and outlook

In 2016 and 2017, Quantum Chemistry of the Excited State has continued its rapid growth observed during the last decades within the group of powerful tools to address photochemical and chemiluminescent studies. Method developments carried out in the period reviewed in the present book chapter point towards an even brighter future for QCEX. Thus, we observe relevant advances achieved which overcome the known limitations of the multiconfigurational quantum-chemistry methods related to the amount of strongly correlated electrons or reduce the computational cost needed to obtain the remaining electron correlation (dynamic correlation). We focus in this review on developments carried out in the DMRG, FCIQMC and semi-stochastic HCI methods to provide with correct wave functions for determining the static electron correlation, and formulations which largely decrease the cost of computing the short-range or dynamical correlation such as the pair natural orbital or frozen natural orbital within the CASPT2 method. Advances are also observed in the computational strategies for obtaining a dynamical description of excited-state phenomena including lifetimes and population distribution in non-adiabatic processes. We highlight in this work improvements

within the quantum dynamics methodologies.

Applications of QCEX methodologies and computational strategies show a progressive trend towards computations on larger-size molecules and systems with a more extended π-conjugation. Illustrative examples are given in the present book chapter in the fields of luminescent materials, molecular rotors, organic optoelectronics, DNA photostability, damage and repair, photosensitisation of biological structures, CL and BL. For instance, works on DNA nucleobases begin to focus more on the competition between distinct excited-state processes in clusters of bases and less on intrinsic properties of the isolated bases which were exhaustively analysed in previous studies. CIX and STCs remains as relevant targets of many QCEX works and shall remain in future studies. The reason is that such quantum-chemistry entities are crucial to correctly interpret many observable properties measured in spectroscopic, photochemistry and CL experiments. The present book chapter also show synergic combinations of QM methods with MM static and dynamic approaches to properly deal with the environmental effects. We also observe that analyses of inter-molecular processes are becoming more common in some fields (DNA photochemistry and photosensitisation) and new in others (CL). In chemiluminescence, we find the first attempt to analyse the inter-molecular catalysed CL mechanism by using multiconfigurational quantum chemistry (CASPT2/CASSCF). Accurate determinations of excited-state inter-molecular phenomena are however still a challenge for protocols which are based on a highly-accurate determination of CASPT2 energies on top of CASSCF optimised structures or for semiclassical dynamics studies based on CASSCF gradients. This is due to the fact that CASSCF is not considering dispersion interactions. Approximate TD-DFT structures or computationally-demanding CASPT2 gradients can be used here, although this is not possible in all cases. In this context, DMRG, FCIQMC, HCI or new and practical corrections of the popular CASSCF method shall be of great relevance.

Acknowledgements

J. S.-M. acknowledges support from the European Commission through the Marie Curie actions (FP8-MSCA-IF, grant nº 747662). D. R.-S. is thankful to the Spanish MINECO/FEDER for financial support through project CTQ2017-87054-C2-2-P and the Ramón y Cajal fellowship with Ref. RYC-2015-19234. A. F.-M. and A. M. are grateful to the French ANR and the Université de Lorraine for their support.

References

[a] *Instituto de Ciencia Molecular, Universitat de València, P.O. Box 22085, 46071 València, Spain. E-mail: Daniel.Roca@uv.es*
[b] *Department of Chemistry, Imperial College London, London SW7 2AZ, UK*
[c] *Université de Lorraine & CNRS, Laboratoire de Physique et Chimie Théoriques, Boulevard des Aiguillettes, BP 70239, 54506, Vandoeuvre-lès-Nancy, France*
[d] *Department of Chemistry, University College London, 20 Gordon Street, London WC1H 0AJ, UK*
[e] *Department of Theoretical Chemistry & Biology, School of Engineering sciences in Chemistry, Biotechnology and Health(CBH), KTH Royal Institute of Technology, SE-10691, Stockholm, Sweden*
[f] *Key Laboratory of Theoretical and Computational Photochemistry, Ministry of Education, College of Chemistry, Beijing Normal University, Beijing 100875, China*

[1] L. Serrano-Andrés, D. Roca-Sanjuán and G. Olaso-González, in Photochemistry, ed. A. Albini, Royal Society of Chemistry, London, 2010, vol. 38, pp. 10–36.
[2] Y.-J. Liu, D. Roca-Sanjuán and R. Lindh, in Photochemistry, ed. A. Albini, Royal Society of Chemistry, London, 2012, vol. 40, p. 42.
[3] D. Roca-Sanjuán, I. Fdez. Galván, R. Lindh and Y.-J. Liu, in Photochemistry, ed. E. Fasani and A. Albini, Royal Society of Chemistry, London, 2015, vol. 42, p. 11.
[4] D. Roca-Sanjuán, A. Francés-Monerris, I. Fdez. Galván, P. Farahani, R. Lindh and Y.-J. Liu, in Photochemistry, ed. E. Fasani and A. Albini, Royal Society of Chemistry, London, 2017, vol. 44, p. 16.
[5] B. O. Roos, in *Adv. Chem. Phys.*, John Wiley & Sons, Inc., 1987, DOI: 10.1002/9780470142943.ch7, pp. 399-445.
[6] F. Aquilante, T. B. Pedersen, R. Lindh, B. O. Roos, A. S. d. Merás and H. Koch, *J. Chem. Phys.*, 2008, **129**, 024113.
[7] D. Escudero, A. D. Laurent and D. Jacquemin, in *Handbook of Computational Chemistry*, ed. J. Leszczynski, Springer Netherlands, Dordrecht, 2016, pp. 1-35.
[8] M. E. Casida and M. Huix-Rotllant, in *Density-Functional Methods for Excited States*, eds. N. Ferré, M. Filatov and M. Huix-Rotllant, Springer International Publishing, Cham, 2016, pp. 1-60.
[9] M. Huix-Rotllant, A. Nikiforov, W. Thiel and M. Filatov, in *Density-Functional Methods for Excited States*, eds. N. Ferré, M. Filatov and M. Huix-Rotllant, Springer International Publishing, Cham, 2016, pp. 445-476.
[10] U. Schollwöck, *Rev. Mod. Phys.*, 2005, **77**, 259.
[11] G. K.-L. Chan and S. Sharma, *Ann. Rev. Phys. Chem.*, 2011, **62**, 465.
[12] S. R. White, *Phys. Rev. Lett.*, 1992, **69**, 2863.
[13] G. Li Manni, S. D. Smart and A. Alavi, *J. Chem. Theory Comput.*, 2016, **12**, 1245.
[14] N. S. Blunt, S. D. Smart, G. H. Booth and A. Alavi, *J. Chem. Phys.*, 2015, **143**, 134117.
[15] G. H. Booth, A. J. W. Thom and A. Alavi, *J. Chem. Phys.*, 2009, **131**, 054106.
[16] A. A. Holmes, C. J. Umrigar and S. Sharma, *J. Chem. Phys.*, 2017, **147**, 164111.
[17] J. E. T. Smith, B. Mussard, A. A. Holmes and S. Sharma, *J. Chem. Theory Comput.*, 2017, **13**, 5468.
[18] E. Tirrito, S.-J. Ran, A. J. Ferris, I. P. McCulloch and M. Lewenstein, *Phys. Rev. B*, 2017, **95**, 064110.
[19] Y. Ma, S. Knecht, S. Keller and M. Reiher, *J. Chem. Theory Comput.*, 2017, **13**, 2533.
[20] Q. Sun, J. Yang and G. K.-L. Chan, *Chem. Phys. Lett.*, 2017, **683**, 291.
[21] H. J. Werner and P. J. Knowles, *J. Chem. Phys.*, 1985, **82**, 5053.
[22] S. Knecht, S. Keller, J. Autschbach and M. Reiher, *J. Chem. Theory Comput.*, 2016, **12**, 5881.
[23] E. R. Sayfutyarova and G. K.-L. Chan, *J. Chem. Phys.*, 2016, **144**, 234301.
[24] P.-Å. Malmqvist and B. O. Roos, *Chem. Phys. Lett.*, 1989, **155**, 189.
[25] P. Å. Malmqvist, B. O. Roos and B. Schimmelpfennig, *Chem. Phys. Lett.*, 2002, **357**, 230.
[26] S. Keller, K. Boguslawski, T. Janowski, M. Reiher and P. Pulay, *J. Chem. Phys.*, 2015, **142**, 244104.
[27] V. Veryazov, P. Å. Malmqvist and B. O. Roos, *Int. J. Quantum Chem.*, 2011, **111**, 3329.
[28] E. R. Sayfutyarova, Q. Sun, G. K.-L. Chan and G. Knizia, *J. Chem. Theory Comput.*, 2017, **13**, 4063.
[29] C. J. Stein and M. Reiher, *J.Chem. Theory Comput.*, 2016, **12**, 1760.
[30] E. G. Hohenstein, N. Luehr, I. S. Ufimtsev and T. J. Martínez, *J. Chem. Phys.*, 2015, **142**, 224103.
[31] J. W. SnyderJr., B. S. Fales, E. G. Hohenstein, B. G. Levine and T. J. Martínez, *J. Chem. Phys.*, 2017, **146**, 174113.
[32] E. G. Hohenstein, *J. Chem. Phys.*, 2016, **145**, 174110.
[33] B. S. Fales, Y. Shu, B. G. Levine and E. G. Hohenstein, *J. Chem. Phys.*, 2017, **147**, 094104.
[34] I. Fdez. Galván, M. G. Delcey, T. B. Pedersen, F. Aquilante and R. Lindh, *J. Chem. Theory Comput.*, 2016, **12**, 3636-3653.
[35] M. G. Delcey, T. B. Pedersen, F. Aquilante and R. Lindh, *J. Chem. Phys.*, 2015, **143**, 044110.
[36] F. Aquilante, M. G. Delcey, T. B. Pedersen, I. Fdez. Galván and R. Lindh, *Mol. Phys.*, 2017, **115**, 2052.
[37] K. Andersson, P.-Å. Malmqvist and B. O. Roos, *J. Chem. Phys.*, 1992, **96**, 1218.
[38] C. Angeli, R. Cimiraglia, S. Evangelisti, T. Leininger and J.-P. Malrieu, *J. Chem. Phys.*, 2001, **114**, 10252.

[39] D. Roca-Sanjuán, F. Aquilante and R. Lindh, *WIREs. Comput. Mol. Sci.*, 2012, **2**, 585.
[40] F. Menezes, D. Kats and H.-J. Werner, *J. Chem. Phys*., 2016, **145**, 124115.
[41] J. Segarra-Martí, M. Garavelli and F. Aquilante, *J. Chem. Theory Comput*., 2015, **11**, 3772.
[42] J. Segarra-Martí, M. Garavelli and F. Aquilante, *J. Chem. Phys.*, 2018, **148**, 034107.
[43] B. Vlaisavljevich and T. Shiozaki, *J. Chem. Theory Comput.*, 2016, **12**, 3781.
[44] M. K. MacLeod and T. Shiozaki, *J. Chem. Phys.*, 2015, **142**, 051103.
[45] J. W. Park and T. Shiozaki, *J. Chem. Theory Comput.*, 2017, **13**, 2561.
[46] D. Ma, G. Li Manni, J. Olsen and L. Gagliardi, *J. Chem. Theory Comput.*, 2016, **12**, 3208.
[47] N. Nakatani and S. Guo, *J. Chem. Phys.*, 2017, **146**, 094102.
[48] T. Yanai, M. Saitow, X.-G. Xiong, J. Chalupský, Y. Kurashige, S. Guo and S. Sharma, *J. Chem. Theory Comput.*, 2017, **13**, 4829.
[49] G. Ghigo, B. O. Roos and P.-Å. Malmqvist, *Chem. Phys. Lett.*, 2004, **396**, 142.
[50] Y. Guo, K. Sivalingam, E. F. Valeev and F. Neese, *J. Chem. Phys*., 2017, **147**, 064110.
[51] Y. Guo, K. Sivalingam, E. F. Valeev and F. Neese, *J. Chem. Phys*., 2016, **144**, 094111.
[52] L. Freitag, S. Knecht, C. Angeli and M. Reiher, *J. Chem. Theory Comput.*, 2017, **13**, 451.
[53] S. Guo, M. A. Watson, W. Hu, Q. Sun and G. K.-L. Chan, *J. Chem. Theory Comput.*, 2016, **12**, 1583.
[54] M. Roemelt, S. Guo and G. K.-L. Chan, *J. Chem. Phys.*, 2016, **144**, 204113.
[55] C. J. Stein, V. von Burg and M. Reiher, *J. Chem. Theory Comput.*, 2016, **12**, 3764.
[56] A. Y. Sokolov and G. K.-L. Chan, *J. Chem. Phys.*, 2016, **144**, 064102.
[57] A. Y. Sokolov, S. Guo, E. Ronca and G. K.-L. Chan, *J. Chem. Phys.*, 2017, **146**, 244102.
[58] S. Sharma, G. Knizia, S. Guo and A. Alavi, *J. Chem. Theory Comput*., 2017, **13**, 488.
[59] S. Sharma, G. Jeanmairet and A. Alavi, *J. Chem. Phys.*, 2016, **144**, 034103.
[60] L. Gagliardi, D. G. Truhlar, G. Li Manni, R. K. Carlson, C. E. Hoyer and J. L. Bao, *Acc. Chem. Res.*, 2017, **50**, 66.
[61] E. D. Hedegård, *Mol. Phys.*, 2017, **115**, 26.
[62] I. Lyskov, M. Kleinschmidt and C. M. Marian, *J. Chem. Phys.*, 2016, **144**, 034104.
[63] A. Heil and C. M. Marian, *J. Chem. Phys.*, 2017, **147**, 194104.
[64] S. Grimme and M. Waletzke, *J. Chem. Phys.*, 1999, **111**, 5645.
[65] M. Filatov, in *Density-Functional Methods for Excited States*, eds. N. Ferré, M. Filatov and M. Huix-Rotllant, Springer International Publishing, Cham, 2016, pp. 97-124.
[66] A. K. Dutta, F. Neese and R. Izsák, *J. Chem. Phys.*, 2016, **145**, 034102.
[67] S. Faraji, S. Matsika and A. I. Krylov, *J. Chem. Phys.*, 2018, **148**, 044103.
[68] E. F. Kjønstad and H. Koch, *J. Phys. Chem. Lett.*, 2017, **8**, 4801.
[69] E. F. Kjønstad, R. H. Myhre, T. J. Martínez and H. Koch, *J. Chem. Phys.*, 2017, **147**, 164105.
[70] J. Brabec, J. Lang, M. Saitow, J. Pittner, F. Neese and O. Demel, *J. Chem. Theory Comput.*, 2018, DOI: 10.1021/acs.jctc.7b01184.
[71] G. W. Richings and G. A. Worth, *Chem. Phys. Lett*., 2017, **683**, 606.
[72] G. W. Richings and S. Habershon, *J. Chem. Theory Comput*., 2017, **13**, 4012.
[73] G. W. Richings and S. Habershon, *Chem. Phys. Lett*., 2017, **683**, 228.
[74] B. F. E. Curchod, C. Rauer, P. Marquetand, L. González and T. J. Martínez, *J. Chem. Phys*., 2016, **144**, 101102.
[75] D. A, Fedorov, S. R. Pruitt, K. Keipert, M. S. Gordon and S. A. Varganov, *J. Phys. Chem. A*, 2016, **120**, 2911.
[76] F. Agostini, S. K. Min, A. Abedi and E. K. U. Gross *J. Chem. Theory Comput*., 2016, **12**, 2127.
[77] S. K. Min, F. Agostini, I. Tavernelli and E. K. U. Gross, *J. Phys. Chem. Lett*. 2017, **8**, 3048.
[78] B. F. E. Curchod and F. Agostini, *J. Phys. Chem. Lett.* 2017, **8**, 831.
[79] M. F. Shibl, J. Schulze, M. J. Al-Marri and O. Kühn, *J. Phys. B: At. Mol. Opt. Phys*., 2017, **50**, 184001.
[80] D. Mendive-Tapia, T. Firmino, H.-D. Meyer and F. Gatti, *Chem. Phys*., 2017, **482**, 113.
[81] J. E. Subotnik, A. Jain, B. Landry, A. Petit, W. Ouyang and N. Bellonzi, *Ann. Rev. Phys. Chem.*, 2016, **67**, 387.
[82] L. Wang, A. Akimov and O. V. Prezhdo, *J. Chem. Phys.*, 2016, **7**, 2100.
[83] ISI Web of Knowledge, Thomson Reuters. http://wokinfo.com.
[84] A. M. El-Zohry, D. Roca-Sanjuán and B. Zietz, *J. Phys. Chem. C*, 2015, **119**, 2249.
[85] L. A. Strada, A. Francés-Monerris, I. Schapiro, M. Olivucci and D. Roca-Sanjuán, *Phys. Chem. Chem. Phys.*, 2016, **18**, 32786.

[86] J. Shi, L. E. A. Suarez, S.-J. Yoon, S. Varghese, C. Serpa, S. Y. Park, L. Lüer, D. Roca-Sanjuán, B. Milián-Medina and J. Gierschner, *J. Phys. Chem. C*, 2017, **121**, 23166.
[87] M. G. S. Londesborough, D. Hnyk, J. Bould, L. Serrano-Andrés, V. Sauri, J. M. Oliva, P. Kubát, T. Polívka and K. Lang, *Inorg. Chem.*, 2012, **51**, 1471.
[88] V. Sauri, J. M. Oliva, D. Hnyk, J. Bould, J. Braborec, M. Merchán, P. Kubát, I. Císařová, K. Lang and M. G. S. Londesborough, *Inorg. Chem.*, 2013, **52**, 9266.
[89] M. G. S. Londesborough, J. Dolanský, L. Cerdán, K. Lang, T. Jelínek, J. M. Oliva, D. Hnyk, D. Roca-Sanjuán, A. Francés-Monerris, J. Martinčík, M. Nikl and J. D. Kennedy, *Adv. Opt. Mat.*, 2017, **5**, 1600694.
[90] M. G. S. Londesborough, J. Dolanský, T. Jelínek, J. D. Kennedy, I. Císařová, R. D. Kennedy, D. Roca-Sanjuán, A. Francés-Monerris, K. Langa and W. Clegg, *Dalton Trans.*, 2018, **47**, 1709.
[91] P. Marquetand, J. J. Nogueira, S. Mai, F. Plasser and L. González, *Molecules*, 2017, **22**, 49.
[92] M. Pola, M. A. Kochman, A. Picchiotti, V. I. Prokhorenko, R. J. D. Miller and M. Thorwart, *J. Theor. Comput. Chem.*, 2017, **16**, 1750028.
[93] L. Martínez-Fernández, A. J. Pepino, J. Segarra-Martí, A. Banyasz, M. Garavelli and R. Improta, *J. Chem. Theory Comput.*, 2016, **12**, 4430.
[94] M. S. Nørby, C. Steinmann, J. M. H. Olsen, H. Li and J. Kongsted, *J. Chem. Theory Comput.*, 2016, **12**, 5050.
[95] R. Improta, F. Santoro and L. Blancafort, *Chem. Rev.*, 2016, **116**, 3540.
[96] J. J. Nogueira, F. Plasser and L. Gonzalez, *Chem. Sci.*, 2017, **8**, 5682.
[97] Z. Benda and P. G. Szalay, *Phys. Chem. Chem. Phys.*, 2016, **18**, 23596.
[98] H. Sun, S. Zhang, C. Zhong and Z. Sun, *J. Comput. Chem.*, 2016, **37**, 6843.
[99] S. Saha and H. M. Quiney, *RSC Adv.*, 2017, **7**, 33426.
[100] A. DeFusco, N. Minezawa, L. V Slipchenko, F. Zahariev and M. S. Gordon, *J. Phys. Chem. Lett.*, 2011, **2**, 2184.
[101] M. Pollum, L. Martinez-Fernandez and C. E. Crespo-Hernandez, in *Photoinduced Phenomena in Nucleic Acids I: Nucleobases in the Gas Phase and in Solvents*, eds. M. Barbatti, A. C. Borin and S. Ullrich, 2015, vol. 355, pp. 245–327.
[102] A. Giussani, J. Segarra-Martí, D. Roca-Sanjuán and M. Merchán, *Top. Curr. Chem.*, 2015, **355**, 57.
[103] J. Segarra-Martí, A. Francés-Monerris, D. Roca-Sanjuán and M. Merchán, *Molecules*, 2016, **21**, 1666.
[104] A. J. Pepino, J. Segarra-Martí, A. Nenov, R. Improta and M. Garavelli, *J. Phys. Chem. Lett.*, 2017, **8**, 1777.
[105] A. J. Pepino, J. Segarra-Marti, A. Nenov, I. Rivalta, R. Improta and M. Garavelli, *Phys. Chem. Chem. Phys.*, 2018, **20**, 6877.
[106] M. Merchan, R. Gonzalez-Luque, T. Climent, L. Serrano-Andres, E. Rodriuguez, M. Reguero and D. Pelaez, *J. Phys. Chem. B*, 2006, **110**, 26471.
[107] R. Gonzalez-Luque, T. Climent, I. Gonzalez-Ramirez, M. Merchan and L. Serrano-Andres, *J. Chem. Theory Comput.*, 2010, **6**, 2103.
[108] L. Martínez-Fernández, A. J. Pepino, J. Segarra-Martí, J. Jovaišaitė, I. Vaya, A. Nenov, D. Markovitsi, T. Gustavsson, A. Banyasz, M. Garavelli and R. Improta, *J. Am. Chem. Soc.*, 2017, **139**, 7780.
[109] D. B. Bucher, B. M. Pilles, T. Carell and W. Zinth, *Proc. Natl. Acad. Sci. U. S. A.*, 2014, **111**, 4369.
[110] L. M. Nielsen, S. V. Hoffmann and S. B. Nielsen, *Photochem. Photobiol. Sci.*, 2013, **12**, 1273.
[111] C. Ko and S. Hammes-Schiffer, *J. Phys. Chem. Lett.*, 2013, **4**, 2540.
[112] D. Roca-Sanjuan, G. Olaso-Gonzalez, I. Gonzalez-Ramirez, L. Serrano-Andres and M. Merchan, *J. Am. Chem. Soc.*, 2008, **130**, 10768.
[113] L. Blancafort and A. A. Voityuk, *J. Chem. Phys.*, 2014, **140**, 95102.
[114] Y. Zhang, X.-B. Li, A. M. Fleming, J. Dood, A. A. Beckstead, A. M. Orendt, C. J. Burrows and B. Kohler, *J. Am. Chem. Soc.*, 2016, **138**, 7395.
[115] K. Rottger, H. J. B. Marroux, M. P. Grubb, P. M. Coulter, H. Bohnke, A. S. Henderson, M. C. Galan, F. Temps, A. J. Orr-Ewing and G. M. Roberts, *Angew. Chemie-International Ed.*, 2015, **54**, 14719.
[116] D. B. Bucher, A. Schlueter, T. Carell and W. Zinth, *Angew. Chemie-International Ed.*, 2014, **53**, 11366.
[117] D. Markovitsi, T. Gustavsson and I. Vayá, *J. Phys. Chem. Lett.*, 2010, **1**, 3271.

[118] V. Ignacio, B. Johanna, H. Miquel, T. A. K., L. F. D., G. Thomas, B. Irene, I. Roberto and M. Dimitra, *Chem. – A Eur. J.*, 2016, **22**, 4904.
[119] M. Huix-Rotllant, J. Brazard, R. Improta, I. Burghardt and D. Markovitsi, *J. Phys. Chem. Lett.*, 2015, **6**, 2247.
[120] J. Cerezo, L. Martínez-Fernández, R. Improta and F. Santoro, *Theor. Chem. Acc.*, 2016, **135**, 221.
[121] C. Rauer, J. J. Nogueira, P. Marquetand and L. González, *J. Am. Chem. Soc.*, 2016, **138**, 15911.
[122] J. I. Mendieta-Moreno, D. G. Trabada, J. Mendieta, J. P. Lewis, P. Gómez-Puertas and J. Ortega, *J. Phys. Chem. Lett.*, 2016, **7**, 4391.
[123] W. Lee, G. Kodali, R. J. Stanley and S. Matsika, *Chem. Eur. J.*, 2016, **22**, 11371.
[124] A. Banyasz, L. Martinez-Fernandez, T.-M. Ketola, A. Muñoz-Losa, L. Esposito, D. Markovitsi and R. Improta, *J. Phys. Chem. Lett.*, 2016, **7**, 2020.
[125] L. Martinez-Fernandez and R. Improta, *Photochem. Photobiol. Sci.*, 2017, **16**, 1277.
[126] A. Giussani, I. Conti, A. Nenov and M. Garavelli, *Faraday Discuss.*, 2018, DOI: 10.1039/C7FD00202E.
[127] J. J. Serrano-Pérez and L. Serrano-Andrés, in *Handbook of Computational Chemistry*, ed. J. Leszczynski, Springer-Verlag, Berlin, 2012, pp. 483–560.
[128] A. Frances-Monerris, J. Segarra-Marti, M. Merchan and D. Roca-Sanjuan, *Theor. Chem. Acc.*, 2016, **135**, 31.
[129] Y. Zhang, K. de La Harpe, A. A. Beckstead, R. Improta and B. Kohler, *J. Am. Chem. Soc.*, 2015, **137**, 7059.
[130] L. Martinez-Fernandez and R. Improta, *Faraday Discuss.*, 2018, DOI: 10.1039/C7FD00195A.
[131] A. Nenov, J. Segarra-Marti, A. Giussani, I. Conti, I. Rivalta, E. Dumont, V. K. Jaiswal, S. F. Altavilla, S. Mukamel and M. Garavelli, *Faraday Discuss.*, 2015, **177**, 345.
[132] Q. S. Li, A. Giussani, J. Segarra-Marti, A. Nenov, I. Rivalta, A. A. Voityuk, S. Mukamel, D. Roca-Sanjuan, M. Garavelli and L. Blancafort, *Chem. Eur. J.*, 2016, **22**, 7497.
[133] J. Segarra-Marti, V. K. Jaiswal, A. J. Pepino, A. Giussani, A. Nenov, S. Mukamel, M. Garavelli and I. Rivalta, *Faraday Discuss.*, 2018, DOI: 10.1039/C7FD00201G.
[134] A. Nenov, A. Giussani, J. Segarra-Marti, V. K. Jaiswal, I. Rivalta, G. Cerullo, S. Mukamel and M. Garavelli, *J. Chem. Phys.*, 2015, **142**, 212443.
[135] A. Giussani, J. Segarra-Martí, A. Nenov, I. Rivalta, A. Tolomelli, S. Mukamel and M. Garavelli, *Theor. Chem. Acc.*, 2016, **135**, 121.
[136] J. Segarra-Martí, A. J. Pepino, A. Nenov, S. Mukamel, M. Garavelli and I. Rivalta, *Theor. Chem. Acc.*, 2018, **137**, 47.
[137] B. Epe, *Photochem. Photobiol. Sci.* 2012, **11**, 98.
[138] J. Nakamura, E. Mutlu, V. Sharma, L. Collins, W. Bodnar, R. Yu, Y. Lai, B. Moeller, K. Lu and J. Swenberg, *DNA Repair (Amst)*, 2014, **19**, 3.
[139] T. J. Dougherty, C. J. Gomer, B. W. Henderson, G. Jori, D. Kessel, M. Korbelik, J. Moan and Q. Peng, *J. Natl. Canc. Inst.*, 1998, **90**, 889.
[140] M. C. Cuquerella, V. Lhiaubet-Vallet, J. Cadet and M. A. Miranda, *Acc. Chem. Res.*, 2012, **45**, 1558.
[141] E. Dumont and A. Monari, *J. Phys. Chem. Lett.*, 2013, **4**, 4119.
[142] E. Dumont, M. Wibowo, D. Roca-Sanjuán, M. Garavelli, X. Assfeld and A. Monari, *J. Phys. Chem. Lett.*, 2015, **6**, 576.
[143] M. Marazzi, M. Wibowo, H. Gattuso, E. Dumont, D. Roca-Sanjuán and A. Monari, *Phys. Chem. Chem. Phys.*, 2016, **18**, 7829.
[144] H. Gattuso, E. Dumont, C. Chipot, A. Monari and F. Dehez, *Phys. Chem. Chem. Phys.*, 2016, **18,** 33180.
[145] M. Marazzi, H. Gattuso and A. Monari, *Theor. Chem. Acc.*, 2016, **135**, 57.
[146] H. Gattuso, V. Besancenot, S. Grandemange, M. Marazzi and A. Monari, *Sci. Rep.*, 2016, **6**, 28480.
[147] A. Penninks, K. Baert, S. Levorato and M. Binaglia, *EFSA J.*, 2017, **15**, 4920.
[148] E. Bignon, M. Marazzi, V. Besancenot, H. Gattuso, G. Drouot, C. Morell, L. A. Eriksson, S. Grandemange, E. Dumont and A. Monari, *Sci. Rep.*, 2017, **7**, 8885.
[149] H. Gattuso, E. Dumont, M. Marazzi and A. Monari, *Phys. Chem. Chem. Phys.*, 2016, **18**, 18598.
[150] V. Vendrell-Criado, G. M. Rodríguez-Muñiz, M. C. Cuquerella, V. Lhiaubet-Vallet and M. A. Miranda, *Angew. Chem. Int. Ed.*, 2013, **52**, 6476.
[151] E. Bignon, H. Gattuso, C. Morell, E. Dumont and A. Monari, *Chem. Eur. J.*, 2015, **21**, 11509.
[152] S. Mai, M. Richter, P. Marquetand and L. González, *Chem. Phys.*, 2017, **482**, 9.

[153] S. Mai, P. Marquetand and L. González, *J. Phys. Chem. Lett.*, 2016, **7**, 1978.
[154] H. Yu, J. A. Sanchez-Rodriguez, M. Pollum, C. E. Crespo-Hernandez, S. Mai, P. Marquetand, L. Gonzalez and S. Ullrich, *Phys. Chem. Chem. Phys.*, 2016, **18**, 20168.
[155] S. Mai, M. Pollum, L. Martínez-Fernández, N. Dunn, P. Marquetand, I. Corral, C. E. Crespo-Hernández and L. González, *Nat. Commun.*, 2016, **7**, 13077.
[156] J. J. Nogueira, M. Meixner, M. Bittermann and L. González, *ChemPhotoChem*, 2017, **1**, 178.
[157] H. Gattuso, M. Marazzi, F. Dehez and A. Monari, *Phys. Chem. Chem. Phys.*, 2017, **19**, 23187.
[158] M. Vacher, I. Fdez. Galván, B.-W. Ding, S. Schramm, R. Berraud-Pache, P. Naumov, N. Ferré, Y.-J. Liu, I. Navizet, D. Roca-Sanjuán, W. J. Baader and Roland Lindh, *Chem. Rev.*, 2018, DOI: 10.1021/acs.chemrev.7b00649.
[159] L. De Vico, Y.-J. Liu , J. W. Krogh and R. Lindh, *J. Phys. Chem. A*, 2007, **111**, 8013.
[160] P. Farahani, D. Roca-Sanjuán, F. Zapata and R. Lindh, *J. Chem. Theory Comput.*, 2013, **9**, 5404.
[161] F. Liu, Y.-J. Liu, L. De Vico and R. Lindh, *J. Am. Chem. Soc.*, 2009, **131**, 6181.
[162] A. Francés-Monerris, I. Fdez. Galván, R. Lindh and D. Roca-Sanjuán, *Theor. Chem. Acc.*, 2017, **136**, 70.
[163] M. Vacher, A. Brakestad, H. O. Karlsson, I. Fdez. Galván and R. Lindh, *J. Chem. Theory Comput.*, 2017, **13**, 2448.
[164] M. Vacher, P. Farahani, A. Valentini, L. M. Frutos, H. O. Karlsson, I. Fdez. Galván and R. Lindh, *J. Phys. Chem. Lett.*, 2017, **8**, 3790.
[165] W. Adam and W. J. Baader, *Angew. Chem. Int. Ed. Engl.*, 1984, **23**, 166.
[166] P. Farahani, M. A. Oliveira, I. Fdez. Galván and W. J. Baader, *RSC Adv.* 2017, **7**, 17462.
[167] M. Stenrup, R. Lindh and I. Fdez. Galván, *J. Comput. Chem.*, 2015, **36**, 1698.
[168] J. P. Zobel, J. J. Nogueira and L. González, *Chem. Sci.*, 2017, **8**, 1482.
[169] P. Farahani and W. J. Baader, *J. Phys. Chem. A*, 2017, **121**, 1189.
[170] F. A. Augusto, A. Francés-Monerris, I. Fdez. Galván, D. Roca-Sanjuán, E. L. Bastos, W. J. Baader and R. Lindh, *Phys. Chem. Chem. Phys.*, 2017, **19**, 3955.
[171] Y.-Y. Cheng and Y.-J. Liu, *Photochem. Photobiol.*, 2016, **92**, 552.
[172] J.-G. Zhou, S. Yang and Z.-Y. Deng, *J. Phys. Chem. B*, 2017, **121**, 11053.
[173] R. Berraud-Pache and I. Navizet, *Phys. Chem. Chem. Phys.*, 2016, **18**, 27460.
[174] E. Coccia, D. Varsano and L. Guidoni, *J. Chem. Theory Comput.*, 2017, **13**, 4357.
[175] Y. Noguchi, M. Hiyama, M. Shiga, O. Sugino and H. Akiyama, *J. Phys. Chem. B*, 2016, **120**, 8776.
[176] C.-G. Min, Y. Leng, Y.-Q. Zhu, X.-K. Yang, S.-J. Huang and A.-M. Ren, *J. Photochem. Photobiol. A: Chem.*, 2017, **336**, 115.
[177] B.-W. Ding and Y.-L. Liu, *J. Am. Chem. Soc.*, 2017, **139**, 1106.
[178] Y. Luo and Y.-J. Liu, *Chem. Eur. J.*, 2016, **22**, 16243.
[179] L. Pinto da Silva, R. F. J. Pereira, C. M. Magalhães and J. C. G. Esteves da Silva, *J. Phys. Chem. B*, 2017, **121**, 7862.
[180] M.-Y. Wang and Y.-J. Liu, *Photochem. Photobiol.*, 2017, **93**, 511.
[181] P. D. Ngo and S. O. Mansoorabadi, *ChemPhotoChem*, 2017, **1**, 383.
[182] L. Pinto da Silva, C. M. Magalhães and J. C. G. Esteves da Silva *ChemistrySelect*, 2016, **1**, 3343.
[183] C.-G. Min, P. J. O. Ferreira and L. Pinto da Silva, *J. Photochem. Photobiol. B*, 2017, **174**, 18.
[184] C.-G. Min, L. Pinto da Silva, J. C. G. Esteves da Silva, X.-K., Yang, S.-J. Huang, A.-M. Ren, Y.-Q. Zhu, *ChemPhysChem*, 2017, **18**, 117.
[185] L. Pinto da Silva, C. M. Magalhaes, D. M. A. Crista and J. C. G. Esteves da Silva, *Photochem. Photobiol. Sci.*, 2017, **16**, 897.